ROBUST OPTION PRICING

by

Mohamed Taik (CID: 01591659)

Department of Mathematics
Imperial College London
London SW7 2AZ
United Kingdom

Thesis submitted as part of the requirements for the award of the MSc in Mathematics and Finance, Imperial College London, 2018-2019

Declaration

The work contained in this thesis is my own work unless otherwise stated.

Signature and date: 10/09/2019

Acknowledgements

I would first like to express my profound gratitude to my thesis supervisor, Dr Pietro Siorpaes, for his enthusiasm, his motivation, and his immense knowledge but especially his devotion to this project. His guidance helped me during all the time of research and writing of my thesis.

I would also like to express my deepest appreciation to the school, Imperial College London, for giving me the chance to be part of this program.

On a more personal level, I would like to give a special thanks to my parents and my brother, who gave me the opportunity to be where I am today, and always encouraged me to do and be better. I am also grateful to my fiance Soraya, for her constant and unconditional support, who stood by me and believed in me throughout this entire journey. Her genuine love gave me the motivation I needed.

Last but not least, I would like to dedicate my paper to my newborn niece Joudy, whose love gave me the inspiration I lacked.

Contents

1 Introduction

Model risk is the risk associated with bad decisions made based on inadequate models. Since the financial crisis in 2008, model risk attracts more and more people working in the financial industry ranging from practitioners to regulators. On the one hand, models can sometime oversimplify reality. For instance, volatility surfaces can not be captured by a simple Black-Scholes model. On the other hand, models might be complex with a significant number of parameters. This can lead to calibration issues such as overfitting.

Motivated by reducing model risk, the aim of this paper is to provide alternative methods to price and hedge financial derivatives. These methods are called "robust" in the sense that they are less exposed to model risk.

This paper is divided into three sections: i) Uncertain volatility models, ii) Martingale Optimal transport problems, iii) Model-independent methods for path-dependent options. The first section describes a robust way to manage volatility without having to assume any deterministic or stochastic model for the volatility process. The second section focuses on understanding optimal transport problems and how they are applicable in mathematical finance in a robust sense. The last section outlines robust methods for some specific path-dependent options: Barrier and Digital options.

The aim is to provide robust upper and lower bounds which contain the actual price almost surely and to compare the results obtained for each method.

1.1 Literature review

The theoretical framework behind uncertain volatility models was mainly studied by Avellaneda, Levy and Parás on [4] and [5]. Their approach is to first explore the general Uncertain Volatility Model (UVM) before introducing the Lagrangian one (λ-UVM) which incorporates more market information.

Optimal transport problems are extensively studied in the Mathematics literature. They were first introduced by Monge [14] and Kantorovich [15] and enhanced recently by Villani [20]. In the financial Mathematics field, this was mainly completed by Henry-Labordere on [3] and Beiglböck, Nutz and Touzi [2] for both discrete and continuous time versions. Guo and Oblój paper [24] offers interesting computational and practical methods for optimal transport problems.

Finally, we will study of robust methods for path-dependent options based on the work of Brown, Hobson and Rogers [27].

Many other research papers are used and will be cited specifically throughout the report.

2 Pricing and hedging derivatives using uncertain volatility models

2.1 Introduction to uncertain volatility models

Volatility is a critical parameter used in pricing and risk-management of financial derivatives. Many attempts were made to estimate this critical variable. In the Black-Scholes model, for instance, we assume the asset to have a constant volatility. This hypothesis is contradicted by actual markets which exhibit stylized facts such as volatility clustering or high persistence. Moreover, the graph of the implied volatility as a function of the strike price exhibits a "smile" shape which cannot be captured by a simple Black-Scholes Model.

Local stochastic volatility models appear to be the solution as they allow a calibration of the volatility surface using the Puts and Calls prices provided by the market. However, Hagan, Kumar, Lesniewski and Woodward [8] notice that these models can generate contradictory results by stating that "*the dynamic behaviour of smiles and skews predicted by local volatility models is exactly opposite of the behaviour observed in the marketplace*".

Another way to proceed is to assume random volatility models, which allow us to estimate multiple paths of the volatility. This could per example be done through autoregressive models such as the ARMA and GARCH ones. However, these methods require a large number of parameters for the calibration, which can lead to overfitting issues.

The uncertain volatility models offer an interesting way to alternatively manage volatility. They are used to price and hedge financial derivatives without having to assume any deterministic or stochastic model for the volatility. Instead, we shall assume that the volatility stands between two extreme values, σ_{min} and σ_{max}, calibrated using historical analysis. Hence, this decreases model risk as less calibration parameters are needed. The only assumption made on volatility is that it lies within a band $[\sigma_{min}, \sigma_{max}]$. However, we are still assuming a model of the form $dS_t = rdt + \sigma_t dW_t$ for the underlying asset: the discounted stock process is therefore a martingale with respect to the filtration of Brownian Motions and it has no jumps.

In this chapter, we will outline the mathematical framework of the uncertain volatility models. We will then focus on how to use options in order to price and hedge other exotic derivatives by using the same framework. Finally, we will highlight its concrete application in the financial markets through several numerical implementations.

2.2 The uncertain volatility model

2.2.1 Assumptions and framework

In this section, we will introduce the statement and the mathematical framework behind the Uncertain Volatility Model (commonly known as the UVM). First, we will consider a derivative security on an underlying stock. We suppose that the stock does not pay any dividends and that it follows a typical stochastic Itô process:

$$\mathrm{d}S_t = \mu_t \mathrm{d}t + \sigma_t \mathrm{d}W_t,$$

where σ_t and μ_t are respectively the spot drift and volatility parameters, and W_t is a Brownian motion. We will only focus on the parameter σ_t and assume that μ_t is constant. Under no arbitrage opportunities, the fundamental theorem of asset pricing implies that under any equivalent martingale measure: $\mu_t = r$ for every t, where r is the risk-free interest rate. The stock price dynamics become:

$$\mathrm{d}S_t = r\mathrm{d}t + \sigma_t \mathrm{d}W_t. \tag{2.1}$$

Concerning the future volatility paths, the only assumption made is that they lie between the values σ_{min} and σ_{max}:

$$\sigma_{min} \leq \sigma_t \leq \sigma_{max}.$$

2.2.2 Calibration of the volatility band

On the one hand, a large volatility band $[\sigma_{min}, \sigma_{max}]$ may lead to unreasonable option prices to be of any practical use. It is therefore important to make the band as small as possible to approximate the price well. On the other hand, an inaccurate calibration of the volatility band $[\sigma_{min}, \sigma_{max}]$ may lead to inadequate prices and thus arbitrage opportunities, which is the reason why the calibration step is crucial. We then face two avenues: either we suppose that the band is time-dependent and deterministic, or we assume that both bounds σ_{min} and σ_{max} are constants.

Let us recall the definition of the Black-Scholes implied volatility for call options:

Definition 2.1. Let C^{mkt} be the market quote price of a call option of maturity T and strike K, r the risk-free interest rate and S_0 the underlying stock price. The implied volatility σ_{imp} is defined as the solution of the equation:

$$BS_{Call}(S_0, K, T, \sigma_{imp}, r) = C^{mkt},$$

where BS_{Call} is the Black-Scholes price formula for Call options.

There is a dependence between the volatility of the stock σ_t and the above implied volatility. In fact, one can demonstrate that supposing a band for the stock volatility equates to supposing a

band for the implied volatility. Let us denote $\sigma_{imp}(t,T)$ the implied volatility of an option at time t and maturity T, one simple choice of a band could be such that:

$$\sigma_{min} \leq \sigma_{imp}(t,T) \leq \sigma_{max}.$$

Hence, if we suppose that the band is constant, a good choice might be that the implied volatility of most liquidly traded options in the market lie within this band.

Otherwise, if we assume the functions $t \mapsto \sigma_{min}(t)$ and $t \mapsto \sigma_{max}(t)$ to be deterministic and time-dependent, a good volatility band could imply that for every $0 \leq t \leq T$:

$$\frac{1}{T-t}\int_t^T \sigma_{min}^2(u)\mathrm{d}u \leq \sigma_{imp}^2(t,T) \leq \frac{1}{T-t}\int_t^T \sigma_{max}^2(u)\mathrm{d}u$$

Simply put, the volatility band can either be deterministic or constant. To calibrate it, one should proceed with a historical analysis: previous option prices provided by the market are considered to be inputs and give us an idea on the "range" of the implied volatilities. These should therefore lie within the volatility band in such a way that it makes it as narrow as possible. We will later on illustrate the effect of the volatility band width on derivatives pricing through numerical examples.

2.2.3 Derivatives pricing under the UVM Model

It is important to understand that for the Uncertain Volatility Model, the option prices are regarded as inputs: we then say that the model is exogenous. Unlike Black-Scholes model for instance (which is an endogenous model), the aim is not to calibrate parameters to price derivative securities but rather to use all the information in the market (mainly Put and Call option prices) to then price exotic options or derive accurate hedging strategies. To clarify the concept, let us consider a derivative security on the underlying stock $(S_t)_{t\geq 0}$. The derivative is supposed to be path-dependent as the cash-flows occur at different settlement dates: $t_1 < t_2 < t_3 < ... < t_N$. Let us denote $F_1(S_{t_1}), F_2(S_{t_2}), F_3(S_{t_3}), ..., F_N(S_{t_N})$ the payoffs due at the previous settlement dates and $\mathcal{P}$ the set of all equivalent martingale measures in order for the process $(S_t)_{t\geq 0}$ to satisfy the equation (2.1). It should be noticed that the set $\mathcal{P}$ is induced by the volatility process and hence depends on the volatility band $[\sigma_{min}, \sigma_{max}]$.

If our calibration of the volatility band is correct, the price of the derivative $V(t,S_t)$ at time $t < t_1$ should lie somewhere between the upper and lower bounds defined as follows:

$$V^+(S_t,t) = \sup_{P\in\mathcal{P}} \mathbb{E}^P\left[\sum_{i=1}^N \mathrm{e}^{-r(t_i-t)}F_i(S_{t_i})\right], \tag{2.2}$$

and

$$V^-(S_t,t) = \inf_{P\in\mathcal{P}} \mathbb{E}^P\left[\sum_{i=1}^N \mathrm{e}^{-r(t_i-t)}F_i(S_{t_i})\right]. \tag{2.3}$$

Avellaneda, Levy and Parás [4] have shown that the above two functions can be obtained by solving partial differential equations (PDE's) with specific boundary conditions. V^+ satisfies:

$$\frac{\partial V^+(S,t)}{\partial t} + r\left(S\frac{\partial V^+(S,t)}{S} - V^+(S,t)\right) + \frac{1}{2}\Sigma_+^2\left[\frac{\partial^2 V^+(S,t)}{\partial S^2}\right] S^2\frac{\partial^2 V^+(S,t)}{\partial^2 S^2} = 0. \tag{2.4}$$

where the operator Σ_+ is defined as:

$$\Sigma_+[X] = \begin{cases} \sigma_{max} & \text{if } X \geq 0. \\ \sigma_{min} & \text{if } X < 0. \end{cases}$$

Similarly, V^- satisfies the following PDE:

$$\frac{\partial V^-(S,t)}{\partial t} + r\left(S\frac{\partial V^-(S,t)}{S} - V^-(S,t)\right) + \frac{1}{2}\Sigma_-^2\left[\frac{\partial^2 V^-(S,t)}{\partial S^2}\right] S^2\frac{\partial^2 V^+(S,t)}{\partial^2 S^2} = 0. \tag{2.5}$$

where this time the operator Σ_- is as follows:

$$\Sigma_-[X] = \begin{cases} \sigma_{max} & \text{if } X \leq 0. \\ \sigma_{min} & \text{if } X > 0. \end{cases}$$

The above non-linear PDE is called the Black-Scholes-Barenblatt equation and is actually a generalization of the classical Black-Scholes PDE, which is obtained with the particular case where $\sigma_{min} = \sigma_{max}$. It should also be noted that to completely determine V^+ or V^-, we need to use a dynamical programming method which comprises specific boundary conditions based on the different cash-flow payoffs $\left(F_i(S_{t_i})\right)_{i\leq N}$. For instance, in the simple case where there is only one settlement date T with a payoff $F(T)$, V^+ is completely determined by solving (2.4) with the boundary condition $V^+(S,T) = F(T)$. The general case will be illustrated numerically later on with a trinomial tree example.

2.2.4 Delta-hedging

In this section, we will briefly outline delta-hedging within the UVM framework. If we define V to be the actual price of the portfolio, we obtain (under an accurate calibration of the volatility band): $V^-(S_t,t) \leq V(S_t,t) \leq V^+(S_t,t)$ for every $t \geq 0$. Hence, under the "worst-case" scenario of the volatility path $(\sigma_t)_{t\geq 0}$, the price of the portfolio would be V^+. The equation (2.4) gives us exactly the volatility path $(\sigma_t^*)_{t\geq 0}$ if this worst-case scenario was to happen:

$$\sigma_t^* = \Sigma_+\left[\frac{\partial^2 V^+(S_t,t)}{\partial S^2}\right].$$

If we assume that the volatility follows this path, then we can use a classical delta-hedging strategy to replicate all future payoffs $\left(F_i(S_{t_i})\right)_{i\leq N}$ of the derivative security: we build a portfolio consisting of long positions on Δ_t shares and B_t bonds, and we dynamically rebalance our positions to satisfy:

$$\Delta_t = \frac{\partial V^+(S_t,t)}{\partial S},$$

and

$$B_t = V^+(S_t, t) - S_t \frac{\partial V^+(S_t, t)}{\partial S}.$$

If we re-use the latter self-financing portfolio in the general case where the volatility is arbitrary and lies within $[\sigma_{min}, \sigma_{max}]$, we will then super-hedge the financial derivative. In fact, if we short the security and we follow the self-financing trading strategy, we will end up with a positive cash-flow after delivering all the payoffs. If the volatility path follows exactly the worst-case scenario $(\sigma_t^*)_{t\geq 0}$, it will then mean we will have perfectly replicated the cash-flow payoffs. Therefore, this is the optimal dynamic hedging strategy that is built using the underlying asset and bonds as hedging instruments. It is optimal since it inevitably generates non-negative cash-flows regardless of the volatility path. A similar reasoning can be applied for the lower bound V^- to hedge a long position on the derivative security.

2.2.5 Hedging with options

Generally, options such as Calls and Puts allow high-order Greek sensitivities (Gamma for instance) through their spot convexity. Thus, we tend to use a portfolio comprising a mix of options as well as the underlying asset to hedge volatility-risk. Intuitively, this is mainly due to the fact that volatilities of the portfolio options tend to cancel each other. Such a phenomenon is known as risk-diversification.

One of the key features of the UVM is that it can capture and quantify this risk diversification. To fix ideas, let us consider a Bank (sell-side) that wishes to market-make a two derivatives portfolio. Let us denote Φ and Θ as their respective discounted payoffs. The upper price V^+ can be seen as the offer price and V^- as the bid price, and $V^+ - V^-$ is therefore the bid-ask spread. Since we have:

$$\sup_{P\in\mathcal{P}} \mathbb{E}^P [\Phi + \Theta] \leq \sup_{P\in\mathcal{P}} \mathbb{E}^P [\Phi] + \sup_{P\in\mathcal{P}} \mathbb{E}^P [\Theta].$$

That means that the offer price of the combined portfolio is reduced compared to the price of each portfolio priced separately. On the other hand, we have:

$$\inf_{P\in\mathcal{P}} \mathbb{E}^P [\Phi + \Theta] \geq \inf_{P\in\mathcal{P}} \mathbb{E}^P [\Phi] + \inf_{P\in\mathcal{P}} \mathbb{E}^P [\Theta].$$

Similarly, the bid price of the combined portfolio is higher than the separate portfolio bid price. Finally, the bid-ask spread is narrowed in the combined portfolio, just as it was expected.

2.3 The Lagrangian Uncertain Volatility Model

Before moving on, let us first summarize the key results we have seen in the Uncertain Volatility Model. We firstly outlined that no assumption related to the volatility paths is made. Following

this, we have then formulated the UVM through the upper (2.2) and lower bounds (2.3) and have seen that those bounds should satisfy the equation (2.1). Finally, we briefly described how to Delta-hedge and super-replicate a portfolio with the UVM as well as how and why hedging with options is more interesting since the model captures risk-diversification. We shall now focus on how to incorporate options market data to the model.

In this section, we will see how to construct efficiently hedging portfolios using option derivatives in addition to the underlying asset. Following [5], we will introduce the Lagrangian Uncertain Volatility Model (known as λ-UVM) as formulated by Avellaneda, Parás and Levy before describing how it is related to the classical Uncertain Volatility Model. Finally, we will explain how to use this model under the trinomial trees framework.

2.3.1 Formulation of the optimization problem

Let us suppose that we want to hedge a short position on a derivative security at time t. We denote Φ the discounted payoff of this derivative and, just as before, $F_1(S_{t_1}), F_2(S_{t_2}), ..., F_N(S_{t_N})$ its cash-flows at the settlement dates $t_1 < t_2 < ... < t_N$:

$$\Phi = \sum_{i=1}^{N} \mathrm{e}^{-r(t_i - t)} F_i(S_{t_i}).$$

Furthermore, let us suppose there are M options (mainly Calls or Puts) in the market which we can use to hedge our position. We denote their payoffs respectively at the maturity dates $t'_1, ..., t'_m$ by $G_1(S_{t'_1}), G_2(S_{t'_2}), ..., G_M(S_{t'_M})$. These options are available in the market at the following prices: $C_1, C_2, ..., C_M$. The main aim is to find the number of option contracts to long or short to efficiently hedge the position. If we denote them by $\lambda_1, \lambda_2, ..., \lambda_M$, we can define the discounted payoff of the hedging portfolio Ψ:

$$\Psi = \sum_{j=1}^{M} \lambda_j \mathrm{e}^{-r(t'_j - t)} G_j(S_{t'_j}).$$

We can further define the expected discounted residual liability L^+ as the maximum payoff loss of the trading strategy:

$$L^+ = \sup_{P \in \mathcal{P}} \mathbb{E}_t^P \left[\Phi - \Psi\right] = \sup_{P \in \mathcal{P}} \mathbb{E}_t^P \left[\sum_{i=1}^{N} \mathrm{e}^{-r(t_i - t)} F_i(S_{t_i}) - \sum_{j=1}^{M} \mathrm{e}^{-r(t'_j - t)} \lambda_j G_j(S_{t'_j}) \right] \tag{2.6}$$

Finally, the total cost of the hedge, defined as $V^+(t, S_t, \lambda_1, ..., \lambda_M)$, is obtained by adding the

above worst-case liability to the cost of the options:

$$\begin{aligned} V^+(t,S_t,\lambda_1,...,\lambda_M) &= L^+ + \sum_{i=1}^{M}\lambda_i C_i \\ &= \sup_{P\in\mathcal{P}} \mathbb{E}_t^P\left[\Phi-\Psi\right] \\ &= \sup_{P\in\mathcal{P}} \mathbb{E}_t^P\left[\sum_{i=1}^{N} \mathrm{e}^{-r(t_i-t)}F_i(S_{t_i}) - \sum_{j=1}^{M}\mathrm{e}^{-r(t'_j-t)}\lambda_j G_j(S_{t'_j})\right] + \sum_{i=1}^{M}\lambda_i C_i \end{aligned} \tag{2.7}$$

Notice that the first term of this equation is similar to the upper bound (2.2) seen in the UVM except that now the payoff incorporates the hedging option prices.

The optimal hedging strategy is the one that minimizes the total hedging cost $V^+(t,S_t,\lambda_1,...,\lambda_M)$; let us call the optimal solution $\widetilde{V}^+(t,S_t,\lambda_1,...,\lambda_M)$. Thus, we are left with the following optimization problem:

$$\widetilde{V}^+(t,S_t,\lambda_1,...,\lambda_M) = \inf_{\lambda_1,...,\lambda_M} V^+(t,S_t,\lambda_1,...,\lambda_M). \tag{2.8}$$

$\widetilde{V}^+$ is therefore the worst-case optimal hedge of a short position of the derivative security. It can thus be seen as an upper bound of the derivative price which should be strictly less than $\widetilde{V}^+$. Indeed, there is equality only when the volatility follows the worst-case scenario. Such an optimization is called the λ-UVM of an upper price. Following [5], if σ_t lies within the volatility band, then the infimum in (2.8) is actually attained.

The steps of deriving the lower bound price of the derivative security are analogous to those for the upper bound. Since we want to hedge a long position on the derivative, the expected discounted residual L^- liability is this time the infimum payoff loss of the trading strategy:

$$L^- = \inf_{P\in\mathcal{P}} \mathbb{E}_t^P\left[\Phi-\Psi\right] = \inf_{P\in\mathcal{P}} \mathbb{E}_t^P\left[\sum_{i=1}^{N} \mathrm{e}^{-r(t_i-t)}F_i(S_{t_i}) - \sum_{j=1}^{M}\mathrm{e}^{-r(t'_j-t)}\lambda_j G_j(S_{t'_j})\right]. \tag{2.9}$$

Similarly, the total cost of the hedging strategy $V^-(t,S_t,\lambda_1,...,\lambda_M)$ is:

$$V^-(t,S_t,\lambda_1,...,\lambda_M) = \inf_{P\in\mathcal{P}} \mathbb{E}_t^P\left[\sum_{i=1}^{N} \mathrm{e}^{-r(t_i-t)}F_i(S_{t_i}) - \sum_{j=1}^{M}\mathrm{e}^{-r(t'_j-t)}\lambda_j G_j(S_{t'_j})\right] + \sum_{i=1}^{M}\lambda_i C_i. \tag{2.10}$$

Keeping in mind that the optimal solution is the one which maximizes the above total cost, let us denote it $\widetilde{V}^-(t,S_t,\lambda_1,...,\lambda_M)$. The optimization problem for the lower bound price therefore becomes:

$$\widetilde{V}^-(t,S_t,\lambda_1,...,\lambda_M) = \sup_{\lambda_1,...,\lambda_M} V^-(t,S_t,\lambda_1,...,\lambda_M) \tag{2.11}$$

Generally, we restrict the number of short and long positions to some boundaries. This is mainly due to liquidity and trading limits constraints. For every i we impose: $\eta_i^- \leq \lambda_i \leq \eta_i^+$ for some constants η_i^+ and η_i^-.

It is worth noting that the hedging developed above for the upper and lower bound price is static, i.e we are taking long or short positions at time t and waiting for the payoffs to happen. However, markets are dynamic and therefore those hedging strategies could be improved by incorporating dynamic strategies and constantly rebalancing the portfolio. In our study, we will only focus on static hedging.

Following [4], the more we increase the number of derivatives used for hedging, the more the upper and lower bound spread ($\widetilde{V}^+ - \widetilde{V}^-$) is narrowed. This is due to the fact that the market tends to become more complete when we increase the number of hedging option instruments. Therefore, it is crucial to work with sufficient Vanilla Calls and Puts data in order to narrow the upper and lower spread price as much as possible.

In a nutshell, we have just outlined how to efficiently derive upper and lower bound prices of a derivative security using options as hedging instruments. Those bounds are respectively given by the optimization problems (2.8) and (2.11). To solve them, we should resolve the UVM problems given by the expected discounted liabilities, (2.6) and (2.9), and pair them with an optimization routine.

2.4 Numerical implementation

2.4.1 Trinomial tree framework

In this section, we shall learn how to solve the optimization problems (2.8) (2.11) under some assumptions of the stock price movements. We assume that after each time step Δt (that can be seen as a trading period), the stock price may reach three different values. Formally if we denote S_t the stock price at time t, then at time $t + \Delta t$, $S_{t+\Delta t}$ might have either one of the following three values: uS_t, mS_t or $\mathrm{d}S_t$ for some constants u,m and d. Graphically:

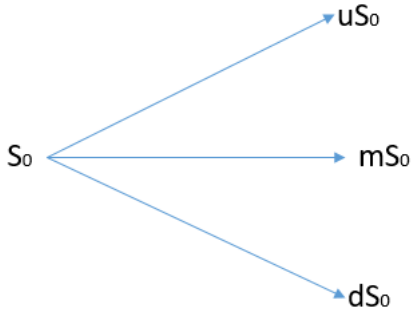

Figure 1: One period trinomial tree

Let us now consider a trinomial tree model with n trading periods, the time horizon of the tree is defined by the final time T and the time step $\Delta t = \frac{T}{n}$. For computational time efficiencies, we impose $ud = m^2$. This condition allows the tree to recombine and therefore avoiding exploding

the total number of nodes. Let us denote the S_i^j by the price of the stock where i the i^{th} time step and j the node price position at this time, with j increases with the price. A three-period trinomial recombined tree is graphically represented as follows:

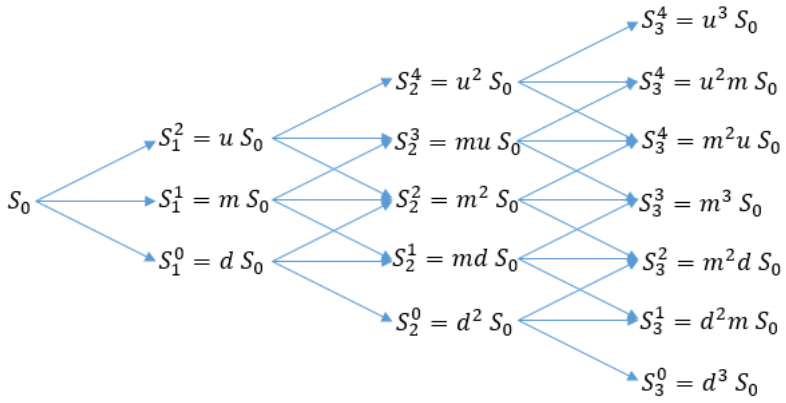

Figure 2: Three period trinomial tree

Notice that at the i^{th} time step, there are $2i+1$ nodes instead of 3^i due to the condition $ud = m^2$. This will considerably reduce the complexity of the numerical implementation algorithm.

As well as developing the uncertain volatility model, Avellaneda, Levy and Parás [5] described how to compute the expected discounted residual liabilities (2.6) (2.9) within the trinomial tree framework. Let us remember that these liabilities are basically the solution of the classical UVM and are obtained by solving the PDE's (2.5) and (2.4). The method used is a finite-difference method.

Let us also notice that, under an accurate choice of u,m and d, the trinomial tree model is incomplete i.e the set $\mathcal{P}$ is not a singleton and contains at least two elements. This is exactly what allows the σ_t to take any value within the volatility band $[\sigma_{min}, \sigma_{max}]$. We should incorporate this degree of freedom within the above model: this is done through the family probability $\{p_u, p_m, p_d\}$ at each node and denotes respectively the probability at which the stock price goes up, towards the center, or down. Intuitively, when the spot volatility is large (say σ_{max}), the stock is more likely to go up or down and therefore p_u and p_d weigh more than p_m. Similarly, if the spot volatility is low (say σ_{min}), the middle probability p_m would weigh more than the two other extreme probabilities.

For the constant parameters u,m and d, we fix:

$$\begin{aligned} u &= \mathrm{e}^{\sigma_{max}\sqrt{\Delta t}+r\Delta t}, \\ m &= \mathrm{e}^{r\Delta t}, \\ d &= \mathrm{e}^{-\sigma_{max}\sqrt{\Delta t}+r\Delta t} \end{aligned} \tag{2.12}$$

We then define the pricing probabilities:

$$\begin{aligned} p_u &= p\left(1 - \frac{\sigma_{max}\sqrt{\Delta t}}{2}\right), \\ p_m &= 1 - 2p, \\ p_d &= p\left(1 + \frac{\sigma_{max}\sqrt{\Delta t}}{2}\right) \end{aligned} \tag{2.13}$$

where the variable p is such that $\frac{\sigma_{min}^2}{2\sigma_{max}} \leq p \leq \frac{1}{2}$ to reflect the above remark about fluctuation probabilities.

2.4.2 Numerical implementation for UVM algorithm

Under the notations (2.12), (2.13), we can easily solve the optimization problems (2.8) and (2.11) of the upper and lower price bounds. Firstly, we need to determine the expected lower and upper liabilities L^+ and L^- by solving the classical uncertain volatility model (2.6) and (2.11). Here, it should be noted that L^+ and L^- are functions of $\lambda_1, ..., \lambda_M$. Then, we need to minimize $\left(L^+(\lambda_1, ..., \lambda_M) + \sum_{i=1}^M \lambda_i C_i\right)$ and maximize $\left(L^-(\lambda_1, ..., \lambda_M) + \sum_{i=1}^M \lambda_i C_i\right)$ with respect to the variables $\lambda_1, ..., \lambda_M$. This can easily be done with classic minimization methods such as the Gradient descent or Powell's method. To that end, we will be using the library *scipy.optimize* from **Python** to proceed with this step.

Let us therefore focus on the first step. To simplify notations, we will write:

$$L^+ = \sup_{P \in \mathcal{P}} \mathbb{E}_t^P \left[\sum_{i=1}^{N'} \mathrm{e}^{-r(t_i - t)} \widetilde{F}_i(S_{t_i}, \lambda_1, ..., \lambda_M) \right], \tag{2.14}$$

and

$$L^- = \inf_{P \in \mathcal{P}} \mathbb{E}_t^P \left[\sum_{i=1}^{N'} \mathrm{e}^{-r(t_i - t)} \widetilde{F}_i(S_{t_i}, \lambda_1, ..., \lambda_M) \right], \tag{2.15}$$

where $N' = max(N, M)$ and, for every i, $\widetilde{F}_i$ is such that:

$$\sum_{i=1}^{N'} \mathrm{e}^{-r(t_i - t)} \widetilde{F}_i(S_{t_i}, \lambda_1, ..., \lambda_M) = \sum_{i=1}^{N} \mathrm{e}^{-r(t_i - t)} F_i(S_{t_i}) - \sum_{j=1}^{M} \mathrm{e}^{-r(t_j - t)} \lambda_j G_j(S_{t'_j}). \tag{2.16}$$

In the first section, we have seen that L^+ and L^- are typically UVM and can be solved using the partial differential equations (2.4) and (2.5). In [9], Parás have developed an algorithm to solve these PDE's within the trinomial tree framework. He also proved the convergence of the solution when the time step Δt tend to 0 (i.e when the number of time periods n of the trinomial tree tends towards infinity).

The algorithm works with a dynamic programming method. We start from the end of the tree and go backward by computing the supremum/infimum of the expected liability i.e to compute the value of L^+ or L^- of each node at time t we use the nodes at time $t+1$. We eventually reach the first node of the tree (at time 0) which corresponds to the current price of the derivative instrument.

Let us denote $W_i^{+,j}$ the value of L^+ of the node in the i^{th} time step positioned in j^{th}, where j is increasing with the price (the notations are similar to those in the Figure 2). $W_i^{-,j}$ is similarly the value of L^- of the node at the (i,j) position. Given n (the number of time steps), T (the final tree time) and $\{u, m, d\}$ (given by the equations (2.12)), we simulate a n period recombined trinomial tree. Following this, we go over each time step corresponding to the settlement dates $t_1, t_2, ..., t_{N'}$ of (2.14) and (2.15) and we substitute each node $S_{t_i}^j$ with its corresponding payoff $\widetilde{F_{t_i}^j} = \widetilde{F}_i(S_{t_i}^j, \lambda_1, ..., \lambda_M)$. At the other times steps we set $\widetilde{F_k^j} = 0$. The tree $(\widetilde{F_i^j})_{\{i,j\}}$ that we obtain will be used to compute the expected liabilities L^+ and L^- while using the algorithm below. For the upper bound L^+:

$$W_i^{+,j} = \widetilde{F_i^j} + \mathrm{e}^{-r\Delta t}\left(W_{i+1}^{+,j} + p_1 L_{i+1}^j\right) \tag{2.17}$$

where

$$L_{i+1}^j = \left(1 - \frac{\sigma_{max}\sqrt{\Delta t}}{2}\right) V_{i+1}^{j+1} + \left(1 + \frac{\sigma_{max}\sqrt{\Delta t}}{2}\right) V_{i+1}^{j-1} - 2V_i^j, \tag{2.18}$$

and p_1 satisfies:

$$p_1 = \begin{cases} 1/2 & \text{if } L_{i+1}^j \geq 0 \\ \sigma_{min}^2/2\sigma_{max}^2 & \text{else..} \end{cases} \tag{2.19}$$

For the lower bound L^-, we have similar results except for (2.19):

$$W_i^{-,j} = \widetilde{F_i^j} + \mathrm{e}^{-r\Delta t}\left(W_{i+1}^{-,j} + p_2 L_{i+1}^j\right), \tag{2.20}$$

where

$$L_{i+1}^j = \left(1 - \frac{\sigma_{max}\sqrt{\Delta t}}{2}\right) V_{i+1}^{j+1} + \left(1 + \frac{\sigma_{max}\sqrt{\Delta t}}{2}\right) V_{i+1}^{j-1} - 2V_i^j,$$

and p_2 satisfies this time:

$$p_2 = \begin{cases} 1/2 & \text{if } L_{i+1}^j < 0 \\ \sigma_{min}^2/2\sigma_{max}^2 & \text{else..} \end{cases} \tag{2.21}$$

All of the process can be summarized in a three step algorithm.

In the first step, the aim is to construct the last step of the payoff tree $(W_i^j)_{i,j}$. We first build the trinomial stock tree and, depending on the values of the last settlement dates of the hedging

instruments and the derivative to hedge, we compute the node values at the last time step. We use the following notations:

- $t_1, ..., t_N$ and $t'_1, ..., t'_M$ are respectively the settlement dates of the hedging option instruments and the derivative to hedge.
- n' is the size of the trinomial tree (which is an input of the user).
- The payoff function F and G are the same of (2.16).
- The function *contruct_trinomial_tree()* construct the stock trinomial tree described above. W_i^j returns the value of the node at the position (i,j).

The pseudo-code of the algorithm for the first step is as follows:

Algorithm 1 Building the last step of the payoff trinomial tree

$m \leftarrow M$
$n \leftarrow N$
W = *construct_trinomial_tree()*
if $t'_m > t_n$ **then**
  for j in 1: 2n'+1 **do**
    $W_n^j = -\lambda_m G_m(W_n^j)$
    $m \leftarrow m - 1$
  end for
else if $t'_m = t_n$ **then**
  for j in 1: 2n'+1 **do**
    $W_n^j = F_n(W_n^j) - \lambda_m G_m(W_n^j)$
    $m \leftarrow m - 1$
    $n \leftarrow n - 1$
  end for
else
  for j in 1: 2n'+1 **do**
    $W_n^j = F_n(W_n^j)$
    $n \leftarrow n - 1$
  end for
end if

In the second step, we will build the whole payoff tree using the equations (2.17), (2.18), (2.19), (2.20) and (2.21). The basic principle of building the tree is, when iterating over all the time steps, to verify whether the payoff of either the hedging instrument or the derivative to hedge occurs. We can this step with the following pseudo-code:

Algorithm 2 Building the whole payoff trinomial tree

$\Delta t = \frac{T}{n'}$

for i in n'-1: 1 **do**

for j in 1: 2i +1 **do**

Given W_{i+1}^j, W_{i+1}^{j+1} and W_{i+1}^{j+2} we set L_{i+1}^j according to equation (2.18).

Set p following (2.19) for the upper bound and (2.21) for the lower bound.

if $i\Delta t \leq t'_m$ or $i\Delta t \leq t_n$ **then**

if $t'_m = t_n$ **then**

$W_i^j = \mathrm{e}^{-r\Delta t}\left(W_{i+1}^{j+1} + pL_{i+1}^j\right) + F_n(W_i^j) - \lambda_m G_m(W_i^j)$

After updating all the node (i.e when $j = 2i+1$) **do**:

$m \leftarrow m-1$

$n \leftarrow n-1$

else if $i\Delta t \leq t'_m$ **then**

$W_i^j = \mathrm{e}^{-r\Delta t}\left(W_{i+1}^{j+1} + pL_{i+1}^j\right) - \lambda_m G_m(W_i^j)$

After updating all the node (i.e when $j = 2i+1$) **do**:

$m \leftarrow m-1$

else

$W_i^j = \mathrm{e}^{-r\Delta t}\left(W_{i+1}^{j+1} + pL_{i+1}^j\right) + F_n(W_i^j)$

After updating all the node (i.e when $j = 2i+1$) **do**:

$n \leftarrow n-1$

end if

else

$W_i^j = \mathrm{e}^{-r\Delta t}\left(W_{i+1}^{j+1} + pL_{i+1}^j\right)$

end if

end for

end for

Let us highlight that the inequalities $i\Delta t \leq t'_m$ and $i\Delta_t \leq t_n$ should rather be equalities. However, when dividing the maximum maturity T into n' small time steps Δt we can encounter the following issue: for n in $\{1, ..., N\}$ there could exist a $k \in \mathbb{N}$ such that $k\Delta t < t_n < (k+1)\Delta t$. In other words, the time steps of the tree could was not able to match perfectly the settlement dates of the derivatives. That is why the above inequalities are used: we force the payoff of a derivative to occur slightly before its true settlement. Also, we can highlight here the importance of the condition $ud = m^2$, which is leading to a recombining trinomial tree and to a quadratic complexity $\mathcal{O}(n'^2)$ instead of an exponential one.

All the variables used in both steps are either inputs from the user or can be deduced from these inputs, except for $\{\lambda_1, ..., \lambda_M\}$ which are more of changing parameters and should solve the

optimization problem (2.11) and (2.8). This is where the ultimate optimization step occurs. If we combine the first and second steps, we can extract the value of the payoff at the initial time W_0^0 as a function of $\{\lambda_1, ..., \lambda_M\}$. We then use a maximization or minimization routine such as gradient descent. For simplicity reasons, we will not detail the optimization step. Recall that $\{C_1, ..., C_M\}$ are the prices of the hedging instruments (options) observed in the market. The algorithm of this last step can now be summarized as follows:

Algorithm 3 Optimization

Get $W_0^0(\lambda_1, ..., \lambda_M)$ using the first two steps.

Set the optimization method

Set limits of long and short positions: for every i in $\{1, ..., M\}$ impose $\eta_i^- \leq \lambda_i \leq \eta_i^+$.

minimize or **maximize** $\left(W_0^0(\lambda_1, ..., \lambda_M) + \sum_{j=1}^{M} \lambda_j C_j\right)$

2.4.3 Application of the UVM: Call options

In this section, we shall explore the numerical implementations of the classical uncertain volatility model in a simple case where the instrument to price/hedge becomes a call option. Let us be reminded that for this model, the only hedging instrument used is the underlying stock. When studying the λ-UVM later on, we will use options as hedging instruments and compare the results of both methods.

We will be using the example of Amazone Call options. The data call prices are taken as quoted in dollars by the NASDAQ Market June 6^{th}, 2019. The spot price of Amazone stock *(AMZN)* is $S_0 = 1746.81$. Let us first and foremost consider the Call options expiring on July 19^{th} , 2019 (i.e in T=43 days). We consider Call prices for a Strike price K ranging from 1515 to 2100. The implied volatility as a function of the Strike price as quoted in the market is represented in figure 3.

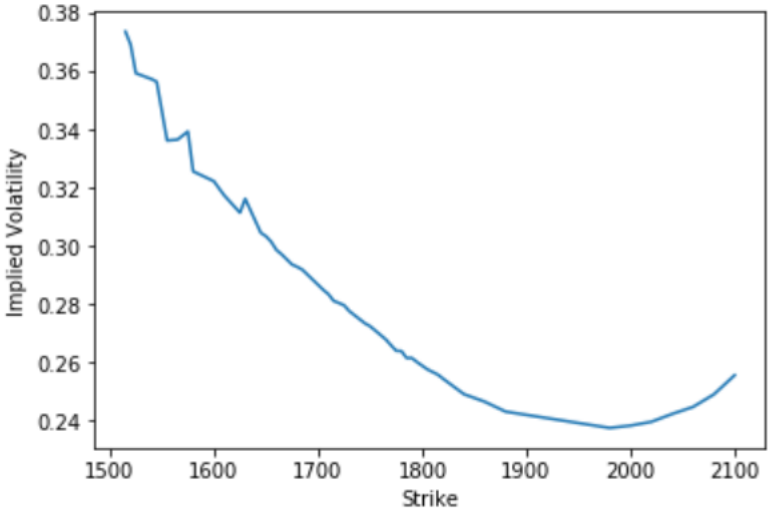

Figure 3: Implied volatility of Call Amazone Options.

A good choice of σ_{min} and σ_{max} would be such that the implied volatility would be contained within such volatility band. Thus, we have chosen $\sigma_{min} = 0.23$ and $\sigma_{max} = 0.4$. Concerning the risk-free interest rate, we use the OIS dollar rate: $r = 0.023$. After solving the equations (2.2) and (2.3) using the numerical algorithm, we obtain the following graph for upper and lower prices:

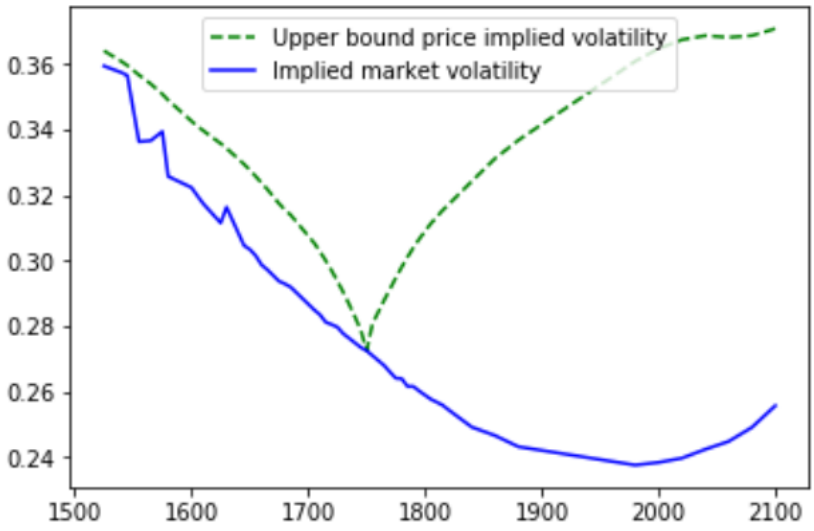

Figure 4: Prices of the UVM upper/lower prices compared to the true market price

To illustrate the effect of the volatility band width, we can plot the same graph, but with two different volatility bands. Let us denote the volatility band 1 by $[\sigma_{min}\ ,\ \sigma_{max}] = [0.23, 0.4]$ (as before) and the volatility band 2 by: $[\sigma_{min}\ ,\ \sigma_{max}] = [0.1, 0.5]$. Figure 5 shows the importance of the volatility band calibration:

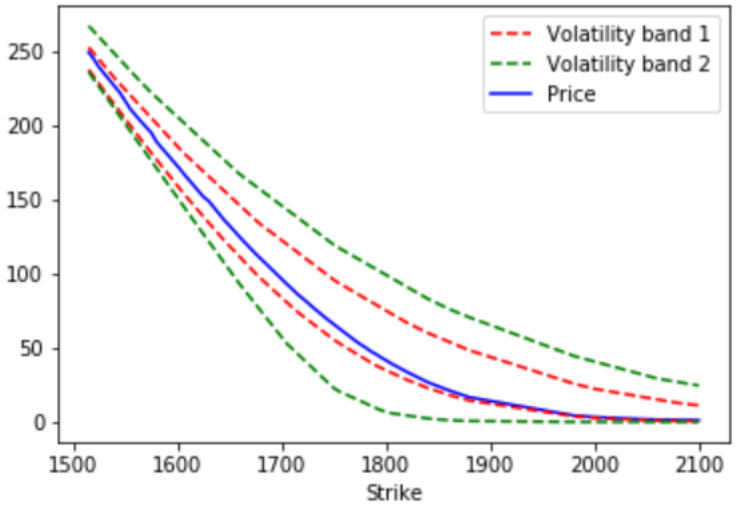

Figure 5: Prices of the UVM upper/lower prices with different calibrated parameters. For band 1, $[\sigma_{min}, \sigma_{max}] = [0.23, 0.4]$. For band 2, $[\sigma_{min}, \sigma_{max}] = [0.1, 0.5]$.

On the one hand, even using a narrow volatility band, the spread between the upper and lower price remains quite high (relatively to actual market bid-ask spreads). Moreover, this spread is bigger for around the money options which lacks coherency with market observations: around the money options are liquidly traded in the market, and both these high supply and demand should narrow the bid-ask spread, which is not the case here.

On the other hand, as seen in the PDE's (2.4) and (2.5), the implied volatilities of the upper and lower prices are respectively functions of the sign of $\frac{\partial^2 V^+(S,t)}{\partial S^2}$ and $\frac{\partial^2 V^-(S,t)}{\partial S^2}$. In this simple case where V^+ and V^- involves one call option (to hedge) and given the fact that the gamma of a call option is known to be positive, it follows that V^+ and V^- are convex functions with respect to the spot price. Using the definition of the operator Σ_+ and Σ_-, the implied volatility of the upper bound price and the lower bound price are respectively σ_{max} and σ_{min}. Therefore, the upper and lower bounds of the UVM are Black-Scholes prices obtained using the extreme volatilities σ_{min} and σ_{max}. This is numerically confirmed in Figure 6, where we plot the implied volatility of the market prices as well as the ones of the upper and lower bound prices of Figure 5.

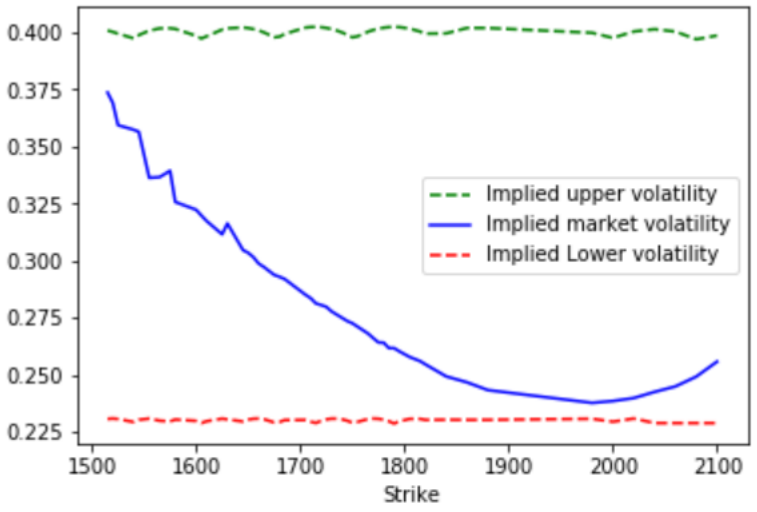

Figure 6: Implied volatilities of the market prices and the upper/lower bound prices

2.4.4 Application of the Lagrangian UVM: Call options

So far, we have numerically implemented the UVM and have witnessed some limitations of this model such as the wide spread between the upper and lower bound for at-the money options as well as the constant-in-time implied volatility. We shall now implement the λ-UVM and verify whether these issues are tackled.

For now let us exclusively use one hedging instrument: an option that expires also in T=43 days with a strike price K=1745, which is the closest strike to the spot price (almost an at the money option). Using notation in (2.16), the only settlement date for both the derivative to hedge and the hedging instrument is $T = t_1 = t'_1$, the hedging payoff function G_1 is equal to $(S_T - K_{ATM})^+$ where $K_{ATM} = 1745$.

After numerically solving the problems (2.14) and (2.15), we obtain the results featuring in Figure 7.

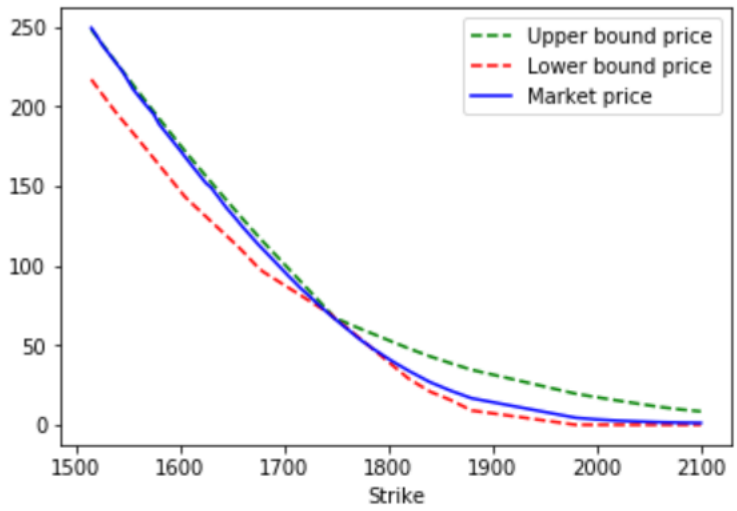

Figure 7: Prices of the λ-UVM upper/lower prices using one hedging instrument

This time, the upper-lower bounds spread has been dramatically reduced, especially for around the money Call option, which is more in line with our expectations.

Let us now focus entirely on the upper bound and study its implied volatility (the same work can be done for the lower bound). The portfolio is slightly more complex than it was before since we allow the combination of short and long option positions by introducing the Call as a hedging instrument. This time, upper prices are not obtained simply by using the extreme volatilities σ_{min} and σ_{max}; it is rather the PDE (2.4) which captures the volatility path that yields the smallest no-arbitrage upper price. This is confirmed in Figure 8 which plots the implied volatility of both the upper prices and the market prices as a function of the strike K.

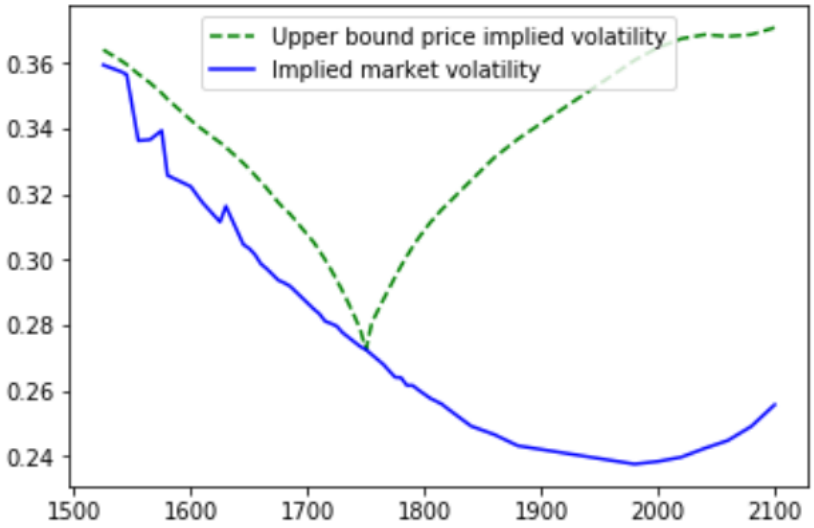

Figure 8: Implied volatilities of market and upper bound prices in the λ-UVM framework

2.4.5 Lagrangian UVM with multiple hedging instruments

As claimed in 2.2.5, the model can quantify risk-diversification. This has been confirmed in the numerical applications above: when we add long or short positions of Call options in the portfolio, we are able to capture a time-dependent implied volatility. We have also noticed that through this risk-diversification, the more hedging instruments we add, the narrower the spread between the upper and lower bound becomes because the volatilities of each instrument in the portfolio tend to cancel each other. Let us illustrate this with a numerical example.

In addition to the hedging Call option used above, we shall now use two other 43-days Call options as hedging instruments. The strikes of these hedging instruments are 1515 and 2100. Their market quotes are featured in Figure 9.

Maturity	Date to maturity (days)	Strike	Market Price
2019-07-19	43	1515	249.33
2019-07-19	43	1745	68.59
2019-07-19	43	2100	1.18

Figure 9: Amazone Vanilla Call options as quoted in the Market the 6^{th} July 2019

After running the numerical algorithm, we can plot the upper bound as before and compare it to market prices:

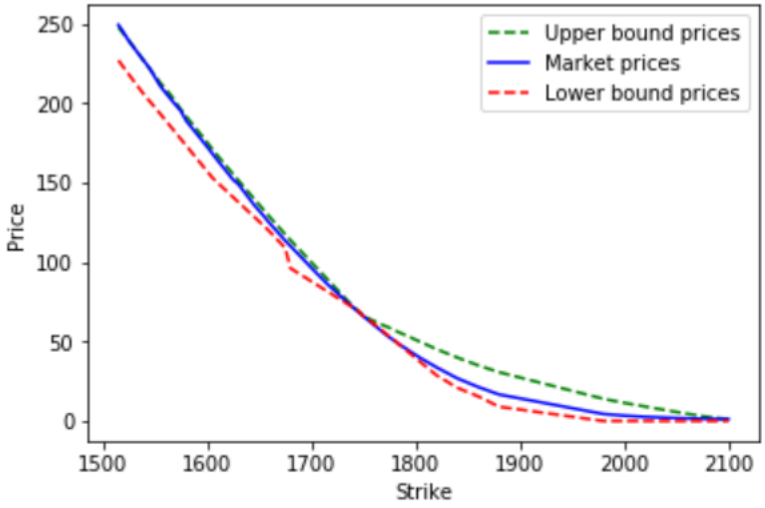

Figure 10: λ-UVM upper and lower bounds using three hedging instruments

We can plot the upper and lower bound spread and see whether incorporating new hedging instruments narrows the spread or not. This is confirmed by Figure 11 as we notice that the spread normalized by the spot price ($\frac{upper-lower}{S_0}$) has decreased when we use two additional hedging instruments.

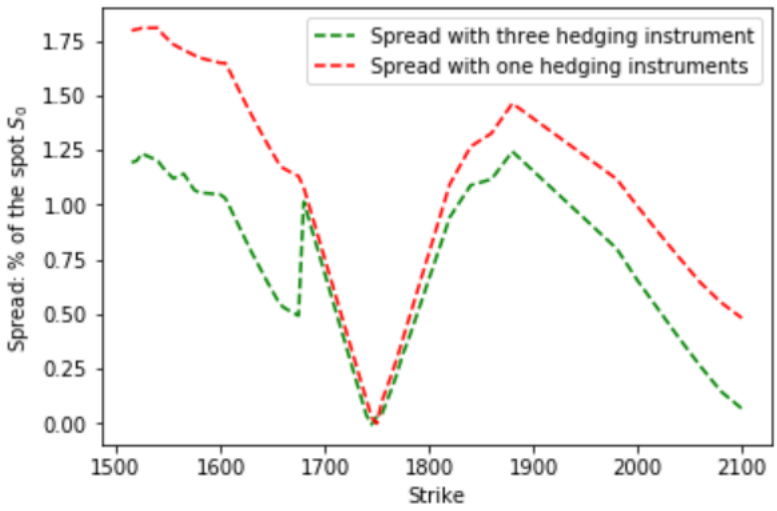

Figure 11: Spread with 3 hedging instruments compared to 1 hedging instrument

2.4.6 Volatility term structures

In this section, we will describe how to induce market information using Call option prices. Instead of pricing derivatives with different Strike prices, we will now fix the Strike price and see how the pricing behaves when changing the maturity T. Mainly, we choose at the money options ($K = S_0$) as they are liquidly traded in the market. Usually, these kind of options are often quoted with their implied volatility. The graph of the implied volatility as a function of the maturity T for at the money options is called the ATM term structure of implied volatility; let us see how the λ-UVM enables its construction.

We shall consider six at-the money options with different maturities as hedging instruments, market quotes are summarized in Figure 12.

Maturity	Date to maturity (days)	Date to maturity (years)	Strike	Price	Implied volatility
2019-06-14	8	0.02192	1745	27.19	0.2504
2019-07-05	29	0.07945	1745	55.48	0.2699
2019-07-19	43	0.11781	1745	68.59	0.2735
2019-10-18	134	0.36712	1740	129.80	0.2892
2020-01-17	225	0.61644	1740	171.50	0.2915
2020-06-19	379	1.03836	1740	235.80	0.3058

Figure 12: Hedging Call options as quoted in the Market the 6^{th} July 2019

The main goal is to use the prices of these ATM hedging instruments to interpolate implied volatilities of ATM options with other Maturities. We will only consider the upper bound case as the lower bound case is similar.

For instance, let us price an ATM option that expiring in 100 days. Intuitively, we can claim that hedging options expiring close to this date (i.e the 43-days and 134-days options) will predominantly be involved in the hedging strategy. Indeed, the optimization algorithm yields an optimal price value of 129.25 with optimal values

$$(\lambda_1, \lambda_2, \lambda_3, \lambda_4, \lambda_5, \lambda_6) = (0, 0.017, 0.259, 0.560, 0.058, 0)$$

as shown in Figure 13.

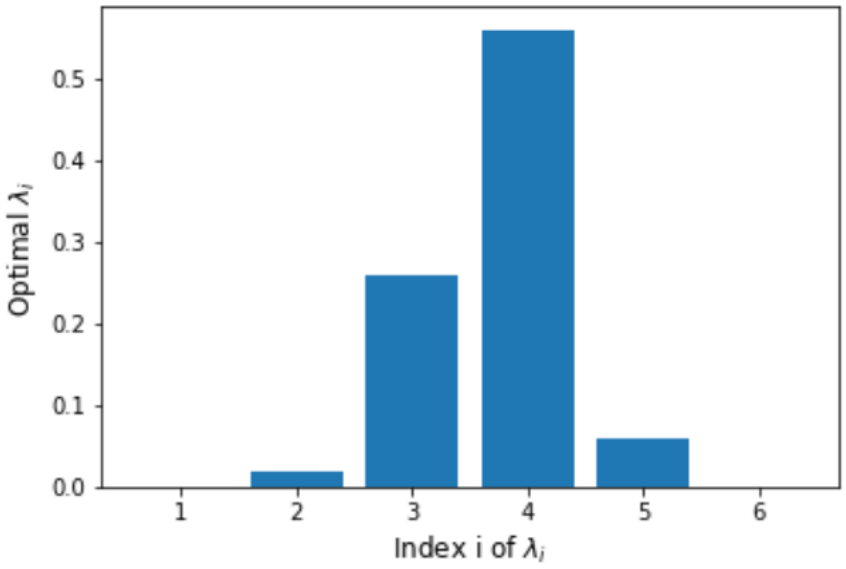

Figure 13: Optimal solutions of pricing an ATM Call option that expires in 100 days

Notice also that it is the hedging option with the next closest maturity (i.e 134-days Call option) which carries the largest hedge part and offers most protection again volatility risk. This is because the other hedging Calls do not offer as much protection as the 134-days Call against volatility risk.

We can plot the ATM implied volatility term structure for a range of maturities. Let us per example choose the following expiry dates: 20, 80, 200, 300, 450, 620 and 730 days. The results summarized in Figure 14 are in line with stylized market observations.

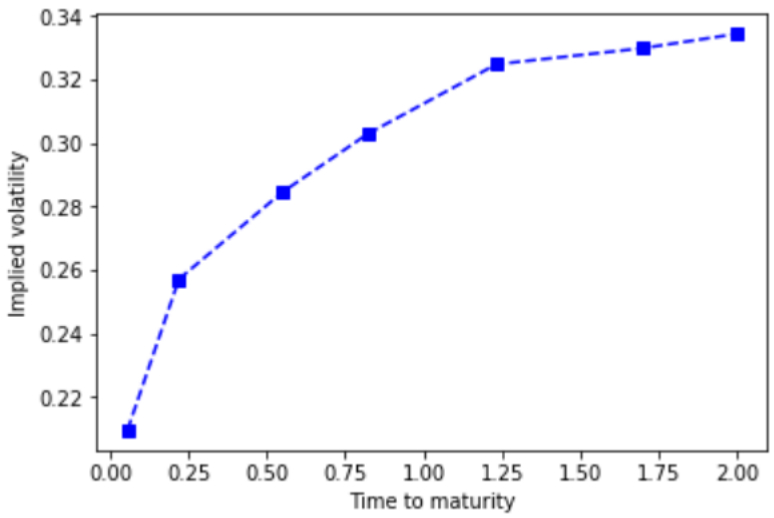

Figure 14: ATM implied volatility term-structure

2.5 Conclusion

In this chapter, we saw an alternative way to manage volatility with uncertain volatility models. Being exogenous, the models incorporate market information (such as Vanilla prices) and calibrate a volatility band. This reduces considerably market risk compared to other statistical or stochastic methods that require more parameters.

We then outlined the importance of using options as volatility hedging instruments, and we saw how the model is able to capture this effect through risk-diversification.

Finally, we tested how the model behaves through concrete numerical applications and saw how to derive important market information such as optimal bid-ask spreads and ATM term structures.

3 Martingale optimal transport problems

3.1 Introduction and context of Optimal transport problems

Optimal Transport problem was first introduced by the French mathematician Monge in 1781 in *Mémoire sur la Théorie des Déblais et des Remblais* [14]. His theory derived from a military transportation problem: he wanted to know how to fill holes with a given pile of sand in the most economic way. In 1940, the Russian mathematician Kantorovic introduced a relaxation of Monge's problem and developed the well-known Monge-Kantorovich optimal transport problem [15]. More recently, Beiglböck, Henry-Labordère and Penkner [16] formulated a link between these optimal transport problems and financial pricing methods.

A market is said to be complete when every future payoff can be replicated using self-financing strategies. The price of the derivative should equate the replication cost under no-arbitrage opportunities. Under market completeness, there exists a unique martingale measure equivalent to the real probability measure. The price of the derivative can be obtained by taking the expectation of the discounted payoff under this equivalent martingale measure. However, when the market is incomplete, there are more than one equivalent martingale measure and the discounted payoff under any of these measures provides a fair price for the derivative.

Let us denote $\mathcal{P}$ as the set of all equivalent martingale measure and $F(X_T)$ as the discounted contingent claim. Hobson [18] suggested that an upper and lower bounds (respectively V^+ and V^-) of the derivative price are naturally obtained as follows:

$$V^+ = \sup_{P \in \mathcal{P}} \mathbb{E}^P \left[F(X_T) \right] \tag{3.1}$$

and

$$V^- = \inf_{P \in \mathcal{P}} \mathbb{E}^P \left[F(X_T) \right] \tag{3.2}$$

However, these bounds may lead to unreasonable prices to be of any practical use. Similarly to what we have seen in the previous chapter, the main idea is therefore to use information in the market (more specifically liquid Vanilla options) to create tighter bounds. Therefore, to price a specific contingent claim, one should use an equivalent martingale measure consistent with the prices of Calls and Puts in the market. This formulation adds a new constraint to the classic optimal transport theory and is called the Martingale Optimal Transport (MOT) problem.

In this Chapter, we will first introduce the classical mathematical theory behind optimal transport problem. Then, we will study the special case of the Martingale optimal transport problem and monitor its application in financial markets through numerical implementations.

3.2 Optimal Transport Problem

3.2.1 Monge-Kantorovich Problem

Let us first offer a general description of Optimal transport problems before highlighting their link with mathematical finance.

Going back to the above military example, we can mathematically model the pile of sand and the holes position respectively by polish sets $\mathcal{X}$ and $\mathcal{Y}$ associated to their Borel sets $\mathcal{B}(\mathcal{X})$ and $\mathcal{B}(\mathcal{Y})$. We then define two probability measures μ and ν on the product set $\mathcal{X}$ x $\mathcal{Y}$.
The transport map T connecting both measures is defined as follows: $T : \mathcal{X} \to \mathcal{Y}$ such that for every B in $\mathcal{B}(\mathcal{Y})$, $\nu(B) = \mu(x \in \mathcal{X}, T(x) \in A)$. Let us here note $\mathcal{T}$ the set of such transport maps (*Remark:* this set could be empty) and, finally, define the cost function $c : \mathcal{X} \times \mathcal{Y} \to \mathbb{R}$.
Intuitively, the measures μ and ν measure respectively the amount of sand and the dimensions of the hole. c(x,y) measures the cost of moving the sand from the point x to y. If we assume the latter to be negative, Monge's problem can be formulated as follows:

Definition 3.1 (Monge optimal transport problem)**.**

$$\mathcal{P}_{monge} = \sup_{T \in \mathcal{T}} \int_{x \in \mathcal{X}} c(x, T(x)) \mu(dx)$$

Notice that the transport map T establishes a bijection between the Borel sets $\mathcal{B}(\mathcal{X})$ and $\mathcal{B}(\mathcal{Y})$. In other words, a pile of sand in the position x has only one specific destination y. If we allow multiple destinations for the specific pile of sand in x, we obtain a relaxation of Monge's Problem commonly known as Monge-Kantorovich Problem.

Formally, Let us denote $\mathcal{P}(\mu, \nu)$ as the set of all probability measures defined on $\mathcal{B}(\mathcal{X}, \mathcal{Y})$, where μ and ν are respectively the first and second marginal laws. For every $\mathbb{P} \in \mathcal{P}(\mu, \nu)$, $A \in \mathcal{B}(\mathcal{X})$ and $B \in \mathcal{B}(\mathcal{X})$, we have $\mu(A) = \mathbb{P}(A \times \mathcal{Y})$ and $\nu(B) = \mathbb{P}(\mathcal{X} \times B)$. Monge-Kantorovich formulation is as follows:

Definition 3.2 (Monge-Kantorovich optimal transport problem)**.**

$$\begin{aligned} \mathcal{P}_{M-K} &= \sup_{\gamma \in \mathcal{P}(\mu,\nu)} \int_{\mathcal{X} \times \mathcal{Y}} c(x, y) \gamma(dx, dy) \\ &= \sup_{\gamma \in \mathcal{P}(\mu,\nu)} \mathbb{E}^{\gamma} \left[c(X, Y) \right] \end{aligned} \tag{3.3}$$

The probabilistic interpretation of Monge-Kantorovich optimal transport problem is that given the cost c and the marginals μ and ν, the aim is the find the best (in the expectation sense) correlation structure.

3.2.2 Duality results

Let us call the above Monge-Kantorovich optimal transport problem the Primal problem. A famous result in optimal transport theory is that this Primal can be dualized. The Dual Monge-

Kantorovich problem is defined as follows:

Definition 3.3 (Dual: Monge-Kantorovich optimal transport problem)**.**

$$\mathcal{D}_{M-K} = \inf_{(\lambda_0,\lambda_1)\in\mathcal{P}^*(\mu,\nu)} \left\{ \mathbb{E}^{\mu}\left[\lambda_0(X)\right] + \mathbb{E}^{\nu}\left[\lambda_1(Y)\right] \right\} \tag{3.4}$$

where $\mathcal{P}^*(\mu,\nu)$ is the set of all function $(\lambda_0,\lambda_1) \in \left(L^1(\mu)\times L^1(\nu)\right)$ such that for every $(x,y)\in\mathbb{R}^2_+$:

$$\lambda_0(x) + \lambda_1(y) \geq c(x,y)$$

We can show that the infimum in (3.3) is actually attained if we ensure that the functions in $\mathcal{P}^*(\mu,\nu)$ are bounded and continuous.

Let us assume that the function $c : \mathbb{R}^2_+ \to [-\infty,\infty)$ is continuous and that there is a constant K such that for every $x \geq 0$ and $y \geq 0$:

$$c^+(x,y) \leq K(1+x+y) \tag{3.5}$$

where c^+ is the positive part of c. Villani [20] have shown that under the assumption (3.5), there is no duality gap (i.e $\mathcal{P}_{M-K} = \mathcal{D}_{M-K}$), which leads to the strong duality theorem commonly known as Kantorovich duality:

Theorem 3.4 (Kantorovich duality)**.**

$$\sup_{\gamma\in\mathcal{P}(\mu,\nu)} \mathbb{E}^{\gamma}\left[c(X,Y)\right] = \inf_{(\lambda_0,\lambda_1)\in\mathcal{P}^*(\mu,\nu)} \left\{ \mathbb{E}^{\mu}\left[\lambda_0(X)\right] + \mathbb{E}^{\nu}\left[\lambda_1(Y)\right] \right\}$$

By the fundamental theorem of asset pricing, the price is obtained by taking the expectation of the discounted payoff under any equivalent martingale measure. However, in the context of optimal transport we consider all the probability measures with given marginals. It is therefore important to add a martingale constraint that is consistent with market data, leading to the Martingale Optimal transport (MOT) problem.

3.3 Martingale optimal transport

3.3.1 Implied marginal distribution by the market

Before formulating the MOT problem, let us first see how to induce marginal distribution from the market.

Breeden and Litzenberger [22] showed that the marginal distribution of an underlying S_T in a specific time T can be induced from the market data using T-Vanilla Calls and Puts prices. Let us fix the maturity T and let the risk-free interest rate r to be equal to zero. Assume also that Call options are known for all strikes $K \geq 0$ and that their prices are obtained using an equivalent martingale measure $\mathbb{Q}$:

$$C(K,T) = \mathbb{E}^{\mathbb{Q}}\left[(S_T - K)^+\right]$$

Then the marginal distribution of S_T implied by the market is obtained as follows:

$$\mathbb{Q}(S_T > \mathrm{d}K) = \frac{\partial C(K,T)}{\partial K} \tag{3.6}$$

and

$$\mathbb{Q}(S_T \in \mathrm{d}K) = \frac{\partial^2 C(K,T)}{\partial K^2} \tag{3.7}$$

This primordial result allows us to incorporate market information within the context of optimal transport. Basically, the main idea is that an optimal upper bound is obtained by using the Monge-Kantorovich problem (3.2) but restraining the set $\mathcal{P}(\mu,\nu)$ to a set of measures where the marginals satisfy the martingale constraint and are implied by the market following the equation (3.7).

3.3.2 Formulation of the two-period discrete time MOT

Before introducing the problem formally, let us first clarify some notations. Instead of working with the two Borel sets $\mathcal{B}(\mathcal{X})$ and $\mathcal{B}(\mathcal{Y})$, we shall work with a fixed probability space $(\Omega, \mathcal{F}, \mathbb{P})$ which is more accurate in a financial context. We shall consider the underlying asset modelled by the stochastic process $(S_t)_{t\in\mathcal{I}}$. Touzi, Beiglböck and Nutz [2] have formulated the problem in the case where $\mathcal{I}$ is an interval. We will mainly study the discrete time version in which $\mathcal{I}$ is a discrete time model.

We mainly focus on a two-period discrete time i.e we want to price a contingent claim $c(s_{t_0}, s_{t_1})$ depending on the price of an underlying asset at two different dates $t_0 < t_1$ (the index time $\mathcal{I}$ is equal to $\{t_0, t_1\}$) . We denote μ_0 and μ_1 the probabilities measures implied by the market satisfying (3.7) with respectively $T = t_0$ and $T = t_1$. Recall that $\mathcal{P}(\mu_0,\mu_1)$ is the set of all probability measures with marginals μ_0 and μ_1 defined on $(\Omega,\mathcal{F})$, we then define $\mathcal{M}(\mu_0,\mu_1)$ to be the set of all possible martingale measure $\mathbb{Q}$ satisfying the marginal constraints imposed by the market:

$$\mathcal{M}(\mu_0,\mu_1) = \left\{\gamma \in \mathcal{P}(\mu_0,\mu_1) : \mathbb{E}^\gamma\left[S_{t_1}|\mathbb{F}_{t_0}\right] = S_{t_0}\right\} \tag{3.8}$$

We will see later on a necessary and sufficient condition to ensure that $\mathcal{M}(\mu_0,\mu_1)$ is not empty.

Finally, the two-period discrete time Martingale Optimal transport problem is given by:

Definition 3.5 (Two-period Martingale Optimal Transport problem)**.**

$$\mathcal{P}_{MOT} = \sup_{\gamma\in\mathcal{M}(\mu_0,\mu_1)} \mathbb{E}^\gamma\left[c(S_{t_1}, S_{t_2})\right] \tag{3.9}$$

Essentially, we have said that the upper bound price (3.1) obtained by taking the supremum over all martingale measures is too large to be of any use. However, if we impose marginals of these martingale consistent with Vanilla prices, we could be able to lower this upper bound since we are incorporating new market information. We have also seen how the problem is closely related to the Monge-Kantorovich optimal transport problem and let us thus study similar duality results.

3.3.3 Formulation of the multi-period discrete time MOT

Suppose now we want to price a path-dependent option which contingent claim $c(S_{t_1}, S_{t_2}, ..., S_{t_n})$ is a function of the underlying asset price at the dates $t_1, ..., t_n$ where $t_1 < t_2 < ... < t_n$. Assume that for every $i \in \{1, ..., n\}$, μ_i are the implied distributions by the market obtained with Vanilla options that expires at t_i and denote $\mathcal{P}(\mu_0, ..., \mu_n)$ the set of all probability measures with given marginals $\mu_1, ..., \mu_n$. A natural extension of the above two-period MOT is to consider the following upper price:

$$\mathcal{P}_{n-MOT} = \sup_{\gamma \in \mathcal{M}(\mu_0, ..., \mu_n)} \mathbb{E}^{\gamma} \left[c(S_{t_0}, S_{t_1}, ..., S_{t_n}) \right] \tag{3.10}$$

Where

$$\mathcal{M}(\mu_0, ..., \mu_n) = \left\{ \gamma \in \mathcal{P}(\mu_0, ..., \mu_n) : \mathbb{E}^{\gamma} \left[S_{t_i} | \mathcal{F}_{t_i} \right] = S_{t_{i-1}}, \quad i = 1, ..., n \right\}$$

Let us now see under which condition the generalized set $\mathcal{M}(\mu_0, ..., \mu_n)$ is non-empty. Given two probability measures μ and ν defined on a particular probability space and with finite first order moment, we state that μ is smaller than ν in the convex order if and only if for every convex function ϕ we have $\mathbb{E}^{\mu}[(\phi(X)] \leq \mathbb{E}^{\nu}[\phi(Y)]$ and we denote $\mu \leq_{cx} \nu$. Strassen's Theorem [21] gives a necessary condition on the existence of a martingale with specific marginal distributions:

Theorem 3.6 (Strassen's Theorem)**.** *Let $(\mu_k)_{0 \leq k \leq n}$ be a family of probability measures on a probability space. There exists a martingale $(S_k)_{0 \leq k \leq n}$ with marginal distributions $(\mu_k)_{0 \leq k \leq n}$ if and only if each for every $k \in \{1, ..., n\}$, μ_k has a finite first order moment and $\mu_i \leq_{cx} \mu_k$ for all $i \leq k$.*

Therefore the set $\mathcal{M}(\mu_0, ..., \mu_n)$ is non-empty if all the probability measures implied by the market are increasing in the convex order as stated in the above theorem. Specifically for the two-period case, $\mathcal{M}(\mu_0, \mu_1)$ is non-empty if and only if $\mu_0 \leq_{cx} \mu_1$.

3.3.4 Duality result for two-period discrete time MOT

The Martingale optimal transport problem is relatively similar to the Monge-Kantorovich optimal transport problem with an additional martingale constraint. At this point, we can ask whether similar duality properties can be derived. Beiglböck, Henry-Labordère and F. Penkner [16] have established a dual version similar to the Monge-Kantorovich one. Let us first consider the two-period problem. Denote $\mathcal{B}$ the set of all continuous and bounded functions on R_+. The Dual of the MOT problem is defined as follows:

Definition 3.7 (Dual: MOT dual formulation)**.**

$$\mathcal{D}_{MOT} = \inf_{(\lambda_0, \lambda_1) \in \mathcal{M}^*(\mu_0, \mu_1), H \in \mathcal{B}} \left\{ \mathbb{E}^{\mu_0} \left[\lambda_0(S_{t_0}) \right] + \mathbb{E}^{\mu_1} \left[\lambda_1(S_{t_1}) \right] \right\} \tag{3.11}$$

where $\mathcal{M}^*(\mu_0, \mu_1)$ is the set of all function $(\lambda_0, \lambda_1) \in \left(L^1(\mu_0) \times L^1(\mu_1)\right)$ such that for every $(s_{t_0}, s_{t_1}) \in \mathbb{R}^2_+$:

$$\lambda_0(s_{t_0}) + \lambda_1(s_{t_1}) + H(s_{t_0})(s_{t_1} - s_{t_0}) \geq c(s_{t_0}, s_{t_1}) \tag{3.12}$$

The main difference with the Monge-Kantorovich dual is the appearance of the bounded function $x \mapsto H(x)$. Following [16], we can derive the MOT duality theorem:

Theorem 3.8 (MOT duality theorem)**.** *Assume have* (3.5) *holds and suppose that μ_0 is smaller than μ_1 in the convex order ($\mu_0 \leq_{cx} \mu_1$), then there is no duality gap i.e:*

$$\mathcal{P}_{MOT} = \mathcal{D}_{MOT} \tag{3.13}$$

The MOT dual can have an intuitive financial interpretation via a semi-static replicating argument. Let us first recall the fact that a European option depending on an underlying asset S with payoff $\lambda(S_T)$ at time T can be statically replicated using bonds, the underlying asset and a strip of T-Vanilla Puts and Calls. Indeed, if we assume that the function λ is twice differentiable, we can prove the following:

$$\lambda(S_T) = \lambda(S_0) + \lambda'(S_0)(S_T - S_0) + \int_0^{S_0} \lambda''(K)(K - S_T)^+ \mathrm{d}K + \int_{S_0}^{\infty} \lambda''(K)(S_T - K)^+ \mathrm{d}K$$

Therefore, we can give the following financial interpretation to the MOT dual formulation:

- $\mathbb{E}^{\mu_0}\left[\lambda_0(S_{t_0})\right] + \mathbb{E}^{\mu_1}\left[\lambda_1(S_{t_1})\right]$ can be interpreted as the price of a replication strategy consisting of: a strip of t_0 and t_1 Vanillas, the underlying asset and bonds.
- $\lambda_0(s_{t_0}) + \lambda_1(s_{t_1})$ is the payoff of the replicating strategy at the settlement dates t_0 and t_1.
- $H(s_{t_0})(s_{t_1} - s_{t_0})$ is the $P\&L$ of the strategy between t_0 and t_1. Indeed, since the replication is semi-static, we are allowed to rebalance the replication portfolio at t_0. We could also add the $P\&L$ between the initial time and t_0, but this term is already incorporated in $\lambda_0(s_{t_0})$.
- $c(s_{t_0}, s_{t_1})$ is the payoff of the contingent claim to price.

It follows that the $\mathcal{D}_{MOT}$ is the minimum replicating price of a portfolio that super-hedges the contingent claim $c(s_{t_0}, s_{t_1})$.

3.3.5 Generalization of the duality result

We can naturally generalize the above duality result in the case where the contingent claim $c(s_{t_0}, ..., s_{t_n})$ depends on the underlying asset at different dates. Let us define the MOT dual formulation for this multi-period version:

Definition 3.9 (MOT dual formulation in the multi-period case)**.** Let $(H_i)_{0\leq i\leq n}$ be a sequence of continuous and bounded function defined on $\mathbb{R}_+^{i+1}$, we have:

$$\mathcal{D}_{n-MOT} = \inf_{(\lambda_0,...,\lambda_n)\in\mathcal{M}^*(\mu_0,...,\mu_n),(H_i(\cdot))_{0\leq i\leq n}} \left\{ \sum_{i=0}^{n} \mathbb{E}^{\mu_i}\left[\lambda_i(S_{t_i})\right] \right\} \tag{3.14}$$

where $\mathcal{M}^*(\mu_0,...,\mu_n)$ is the set of all functions $(\lambda_0,....,\lambda_n) \in \left(L^1(\mu_0)\times ...\times L^1(\mu_n)\right)$ so that for every $s_{t_i}\geq 0$:

$$\sum_{i=0}^{n}\lambda_i(s_{t_i}) + \sum_{i=1}^{n-1} H(s_{t_0},...,s_{t_i})(s_{t_{i+1}-s_{t_i}}) \geq c(s_{t_0},...,s_{t_n})$$

The financial interpretation of the multi-period dual is the same as the two-period case. Notice that H_i representing the rebalancing of the semi-static portfolio at t_i is naturally a function of all previous asset prices up until the date t_i. As before, the replicating portfolio consists of t_i-Vanillas for every $i\in\{0,...,n\}$, the underlying asset, as well as cash.

3.4 Numerical implementation

The questions now arising are the following: how to solve and find the optimal solutions for both the primal and dual of MOT problems? Which one is easier to solve? Are there numerical techniques that we can implement?

P. Henry-Labordère and N. Touzi [23] have shown that for particular payoffs c, the MOT could be solved analytically using stochastic control or Shorokhod embedding techniques. However, for general payoffs numerical and computational techniques are needed. G.Guo and J. Oblój [24] have introduced several computational methods to solve MOT problems for both the discrete and continuous time versions. In this chapter, we will mainly focus on discrete time numerical methods and we will see how MOT problems can be estimated using Linear programming methods.

For simplicity, we will only focus on pricing contingent claims depending on the underlying asset at two different dates i.e we will only study the two-period discrete time MOT. Furthermore, we assume that the assumption (3.5) remains for the rest of the chapter.

3.4.1 Solving numerically the MOT primal

Let us study the Primal case first, to solve this problem we firstly need the implied probability measures μ_0 and μ_1 from the quoted prices of Vanillas for all strikes K. However in practice, not all strikes are traded in the market. We therefore need to interpolate the available Vanillas values in the market to obtain the prices for the entire spectrum of strikes. This step is called the interpolation step and will not be discussed in detail.

If we assume that μ_0 and μ_1 are increasing in the convex order, then following the MOT duality theorem, there is no duality gap. Therefore, there are mainly two ways to proceed: we can either find the optimal value of the Primal MOT or the the Dual MOT, and both results should be equal.

Assuming that we are working for prices in the real line $\mathbb{R}_+$, Monge-Kantorovich optimal value is obtained minimizing:

$$\int_{\mathbb{R}_+^2} c(x,y)\mathbb{P}(dx,dy) \tag{3.15}$$

where $\mathbb{P}$ is a probability measure with given marginals μ_0 and μ_1, i.e for every E in the real positive Borel set $\mathcal{B}_+(\mathbb{R})$ we have:

$$\mathbb{P}\left[E \times \mathbb{R}_+\right] = \mu_0(E) \tag{3.16}$$

and

$$\mathbb{P}\left[\mathbb{R}_+ \times E\right] = \mu_1(E) \tag{3.17}$$

The additional martingale constraint which leads to the Martingale optimal transport is reflected by the following equation:

$$\int_{\mathbb{R}_+} y\mathbb{P}_y(dy) = x, \quad x \in \mathbb{R}_+ \tag{3.18}$$

where $\mathbb{P}_y$ is the restriction of $\mathbb{P}$ to the second marginal distribution.

Let us discretize the value of the underlying asset at t_0 and t_1. We assume that this asset can take n values $x_1, ..., x_n$ at time t_0 and m values $y_1, ..., y_m$ at time t_1. We therefore generate a two-dimensional grid $n \times m$ corresponding to the possible underlying price at two different times.

Similarly, we would like to discretize μ_0 and μ_1 into respectively n and m values to obtain $(\mu_0^i)_{1\leq i\leq n}$ and $(\mu_1^j)_{1\leq j\leq m}$. However, the discretization of the implied probability measures without loosing certain properties is not as easy as it appears. In fact, as Baker [1] pointed out, there are many methods to approximate a probability measure by a discrete measure (commonly known as quantizing the measure), but most of them fail to preserve the increasing convex order which is important in our case for no duality gap. Baker further explained how the so-called $\mathcal{U}$-quantization succeeds to preserve the convexity increasing order. We shall therefore use the latter method to quantize the implied probability measure μ_0 and μ_1.

Finally discretizing the equations (3.15), (3.16), (3.17) and (3.18) as well as the implied probability measures lead to the following linear program for solving the Primal problem:

$$\max_{(p_{i,j})_{1\leq i\leq n, 1\leq j\leq m}} \sum_{i=1}^{n}\sum_{j=1}^{m} p_{i,j}c(x_i,x_j) \tag{3.19}$$

subject to:

$$\sum_{j=1}^{m} p_{i,j} = \mu_0^i, \quad i = 1, ..., n$$
$$\sum_{i=1}^{n} p_{i,j} = \mu_1^j, \quad j = 1, ..., m$$
$$\sum_{j=1}^{m} p_{i,j} y_j = \mu_0^i x_i, \quad i = 1, ..., n$$

This linear program can easily be solved numerically using the Simplex algorithm. Finally, we summarize the numerical steps of the algorithm as follows:

Step 1: Interpolate the available t_0-Vanilla and t_1-Vanilla options to obtain the prices for all strikes

Step 2: Using (3.7), deduce the implied measure distributions μ_0 and μ_1.

Step 3: Discretize the underlying asset at t_0 and t_1 with respectively n and m values.

Step 4: Using $\mathcal{U}$-quantization, approximate μ_0 and μ_1 by discrete measures that can take respectively n and m values.

Step 5: Solve the Linear Program (3.19).

3.4.2 Solving numerically the MOT dual

As we will see in this section, Solving the MOT Dual (3.11) is slightly easier than solving the MOT primal. Indeed, no interpolation and quantization steps are needed. In [3], Henry-Labordère proposed to solve the MOT Dual using also linear programming.

The main idea is to approximate (see section 4.3.4) $\mathbb{E}^{\mu_0}[\lambda_0(S_{t_0})] + \mathbb{E}^{\mu_1}[\lambda_1(S_{t_1})]$ by a weighted sum of prices of Calls available in the market, cash and the underlying stock (Recall that the risk-free interest rate r equals zero):

$$\mathbb{E}^{\mu_0}[\lambda_0(S_{t_0})] + \mathbb{E}^{\mu_1}[\lambda_1(S_{t_1})] \approx \alpha S_0 + \beta + \sum_{l=1}^{N} \omega_0^l C(t_0, K_0^l) + \sum_{k=1}^{M} \omega_1^k C(t_1, K_1^k),$$

where $C(t_0, K)$ and $C(t_1, K)$ are the market values of a call of maturities respectively t_0 and t_1 and strike K.

As before, we then proceed to a discretization of the underlying price at t_0 with n possible values $(x_i)_{1 \le i \le n}$ and at t_1 with m possible values $(y_j)_{1 \le j \le m}$. The constraint (3.12) can be discretized as well: for all $i \in \{1, ..., n\}$ and $j \in \{1, ..., m\}$

$$\alpha S_0 + \beta + \sum_{l=1}^{N} \omega_0^l (x_i - K_0^l)^+ + \sum_{k=1}^{M} \omega_1^k (y_j - K_1^k)^+ + \theta x_i (y_j - x_i) \ge c(x_i, y_j)$$

for some $(\alpha, \beta, \theta) \in \mathbb{R}^3$.

the dual (3.11) can therefore be approximated by the minimization of a linear objective function with respect to $n \times m$ constraints. This leads to the following linear program which approximates the upper bound:

$$\min_{\alpha,\beta,\mu,\omega_0^l,\omega_1^k} \alpha S_0 + \beta + \sum_{l=1}^{N} \omega_0^l C(t_0, K_0^l) + \sum_{k=1}^{M} \omega_1^k C(t_1, K_1^k) \tag{3.20}$$

subject to, for every $i \in \{1, ..., n\}$ and $j \in \{1, ..., m\}$:

$$\alpha S_0 + \beta + \sum_{l=1}^{N} \omega_0^l (x_i - K_0^l)^+ + \sum_{k=1}^{M} \omega_1^k (y_j - K_1^k)^+ + \theta x_i (y_j - x_i) \geq c(x_i, y_j) \tag{3.21}$$

The lower bound is obtained by replacing in the above linear program "min" by "max" and "$\geq$" by "$\leq$" in (3.21).

3.4.3 Numerical examples

In this section, we will illustrate a simple numerical implementation of the previous Dual linear program.

Our aim is the price the following contingent claim: $c(S_{t_0}, S_{t_1}) = (S_{t_0} S_{t_1} - K)^+$ where $t_0 = 0.5$ and $t_1 = 1$, and S_{t_i} the underlying price at t_i. Suppose also that the spot price is initially $S_0 = 1$. This time we do not use real market data, we rather simulate a volatility surface using the SSVI model [28]. The parameters of the later model are chosen randomly but in a way to be consistent with real market behaviour. We assume that the stock price at t_0 and t_1 is the Black-Scholes price obtained with the implied volatility structure of the SSVI model at these dates (Figure 15).

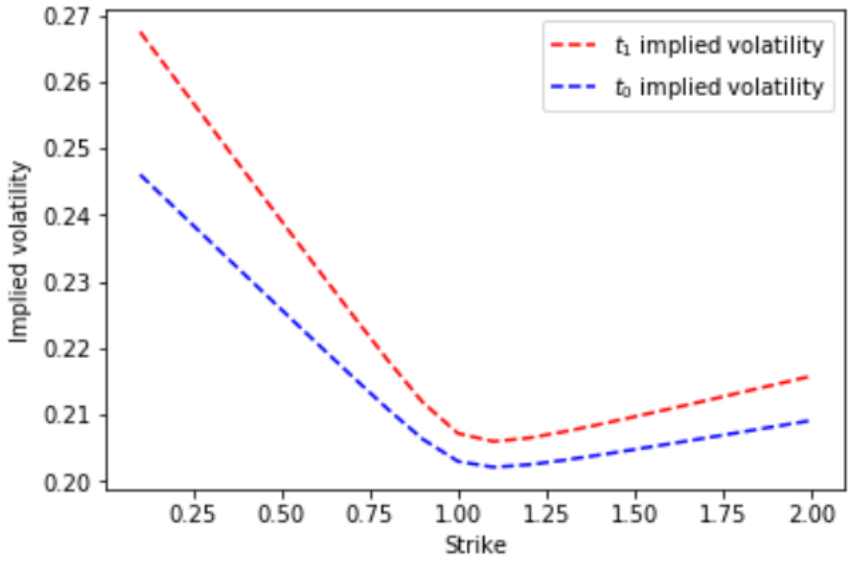

Figure 15: Implied volatility structure obtained with the SSVI model at t_0 and t_1

We use the same notations as the ones of previous section (3.4.2). We assume that the Vanilla Calls are quoted on the market with 20 strikes in $[0, 2]$ at t_0 and t_1 (N = M = 20). Finally, we assume that the underlying can take 10 different values in $[0, 2]$ and we discretize S_{t_0} and S_{t_1} on a two-dimensional grid of 100 values. After solving the linear program (3.20) with the constraints (3.21) for the upper and lower bound, we obtain the results shown in figure 16.

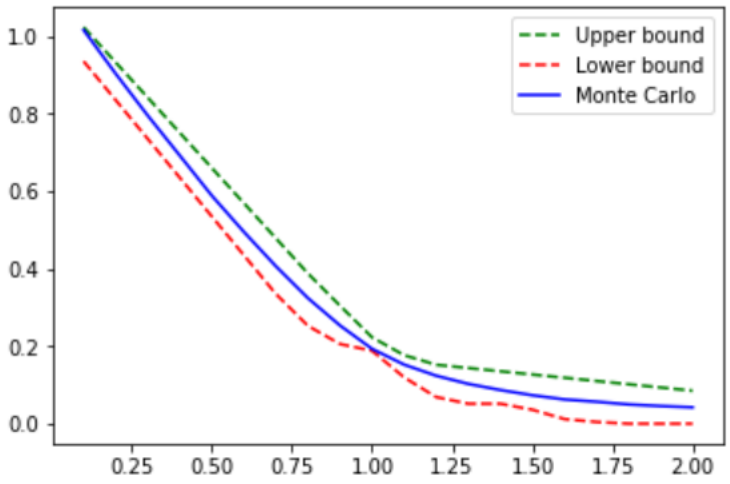

Figure 16: MOT linear program results

To verify our results, we simulated for each strike the price of the contingent claim using Monte-Carlo to find out that the result indeed lies within the upper and lower bounds.

Finally, we compare the upper and lower bound spread to the one obtained with λ-UVM using $\sigma_{min} = 0.22$ and $\sigma_{max} = 0.35$. These results are delivered in Figure 17.

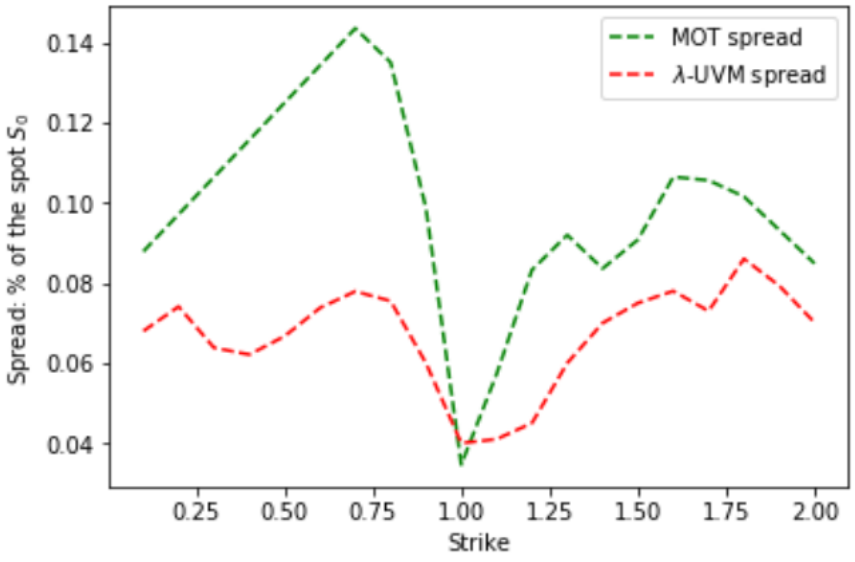

Figure 17: Spread obtained with λ-UVM and MOT

λ-UVM results seem to be more optimal than those obtained with MOT. This might be due to several reasons: firstly, the linear programming approximation might be too brutal; secondly, λ-UVM is less robust than MOT, in the sense that it is based on more assumptions (on the underlying stock process and the calibration of $[\sigma_{min}, \sigma_{max}]$), which therefore leads to tighter bounds. We refer to [3] and [2] for continuous time MOT versions which lead to even tighter spreads and thus better results.

3.5 Conclusion

In this chapter, we introduced Optimal transport problems and derived important Duality results. We then formulated similar problems but with an additional martingale constraint called MOT.

We also derived Duality results for MOT and outlined a few numerical techniques to solve discrete-time versions with linear programming.

Finally, we illustrated how to price a two-period contingent claim by solving numerically the MOT Dual, and we compared our results with those obtained using λ-UVM.

4 Alternative model-independent methods for path-dependent options

4.1 Introduction

In this Chapter we will study alternative model-independent methods to price some path-dependent derivatives, more specifically digital and barrier options. The philosophy used here is quite similar to previous chapter: the aim is to derive the optimal upper and lower bounds consistent with market data to price digital and barrier options.

We shall assume that the risk-free interest rates are zero. Furthermore, we make the idealistic assumption that Calls and Puts with all possible strikes are available in the market, this can be obtained in practice with an interpolation routine.

Unlike uncertain volatility models, no assumption is needed concerning the behaviour of the underlying asset and the calibration of the volatility band. We will see how the knowledge of Vanilla prices is sufficient to produce optimal bounds for digital and barrier options. The method to calculate these bounds is based upon simple replicating strategies.

Since we work under a zero-interest-rates framework, the process of the underlying asset is a martingale with respect to the filtration of Brownian Motion. The main idea is to exhibit (astutely) upper and lower bound prices based on hedging strategies, then to verify that these bounds are indeed optimal by exhibiting martingales for which these bounds are attained. These martingales should also be in compliance with market data. The idea is quite similar to the volatility best and worst case scenarios seen in the uncertain volatility models in the sense that here we look for the minimum or maximum possible martingale laws.

The structure of the chapter is articulated as follows. Firstly, we will discuss the simple example of pricing a path-dependent digital option. Then, we will mainly focus on the core part which is pricing knock-in and knock-out barrier options. Finally, we will outline our results with some numerical examples.

4.2 Digital options

Let us fix the maturity T (say T = 1 year) and Call C(K) the prices of Calls with maturity T and Strike K. Following section 3.3.1, we define μ the implied law of the underlying asset $(S_t)_{t\geq 0}$ at time T i.e for each strike $K \geq 0$, μ satisfies:

$$C(K) = \int (x-K)\mu(dx)$$

Assume that all Calls with all strikes are available in the market and that $x \to C(x)$ is twice differentiable, then $\mu(dx) = C''(x)dx$. Throughout the chapter, we denote $\mathbb{P}$ and $\mathbb{E}$ respectively the probability and the expectation associated to the implied measure μ. For instance, a binary

option which payoff at T is $\mathbb{1}_{\{S_T \geq B\}}$ where B is a constant barrier, the price of this option is $\mathbb{E}(\mathbb{1}_{\{S_T \geq B\}}) = \mathbb{P}(S_T \geq B) = \mu([B, \infty))$.

Digital options also have an unit payoff. However, unlike Binary options, Digital options are path-dependent options i.e their payoff at T depends on the value of the underlying asset before this time. If the underlying asset price crosses a fixed Barrier B before T, the unit payoff occurs; otherwise, the payoff is null. Formally, the payoff of a digital option is $\mathbb{1}_{\{H_B \leq T\}}$ where $H_B = \inf_{t \geq 0}(S_t \geq B)$

To find the upper bound price of the digital option, the main idea is to find an upper bound of the payoff small enough to be the optimal upper bound. Similarly for the lower bound, we should find a lower bound big enough to be optimal. These bounds are derived using the so-called martingale inequalities based on the work of Gilat and Dublins [25] and Hobson [26].

Let us firstly derive the optimal lower bound of a digital option.

Proposition 4.1. *Let $B > S_0$. The optimal Lower bound consistent with market data of a digital option is given by :*

$$L_{dig} = -C'(B) \tag{4.1}$$

where C(K) is the market Call price with maturity T and strike K. If we assume that the underlying asset process is a continuous martingale, then we can improve the previous bound by adding a positive term, the new lower bound is given by:

$$L'_{dig} = -C'(B) + \sup_{K<B} \frac{C(B) - P(K)}{B - K} \tag{4.2}$$

Proof. Let us first prove the result in the general case where no continuity assumption of the martingale $(S_t)_{t \geq 0}$ is made. The first step is to show that for any martingale $(S_t)_{t \geq 0}$ with S_0 given and S_T has law μ (i.e in line with available market Call prices), the price obtained of the digital option is above -C'(B). The second step is to exhibit a martingale such that the lower bound -C'(B) is attained and therefore becomes the optimal lower bound.

Let $(S_t)_{t \geq 0}$ be any martingale so that S_T has law μ. We trivially have $\mathbb{1}_{\{H_B \leq T\}} \geq \mathbb{1}_{\{S_T \geq B\}}$ since $\{H_B \leq T\} \supseteq \{S_T \geq B\}$. Taking expectations we obtain:

$$\mathbb{P}(H_B \leq T) \geq \mathbb{P}(S_T \geq B) = \mu([B, \infty] = -C'(B)$$

Now take the martingale $(S^*_t)_{t \geq 0}$ such that $S^*_t = 1$ for every $t < T$ and with a jump at time T so that S^*_T has law μ. With this specific martingale the inequality $\mathbb{P}(H_B \leq T) = -C'(B)$ holds. Therefore L_{dig} is the best lower bound we can obtain.

Let us see the case where we assume that the underlying asset process is continuous, so that if the Barrier is attained, the underlying price equals it. This time we will be using the following inequality, for every $K < B$:

$$\mathbb{1}_{\{H_B \leq T\}} \geq \mathbb{1}_{\{S_T \geq B\}} + \frac{(S_T - B)^+}{B - K} - \frac{(K - S_T)^+}{B - K} + \frac{B - S_T}{B - K}\mathbb{1}_{\{H_B \leq T\}}$$

The above inequality can be easily proven by distinguishing the cases where the barrier has been reached from the cases it has not. If not reached, the left hand side (LHS) equals zero and the right hand side (RHS) equals $-\frac{(K-S_T)^+}{B-K}$, however, which is not positive. If the Barrier is reached then the LHS is equal to 1 and the RHS is equal to $\mathbb{1}_{\{S_T \geq B\}} + \frac{(B-S_T)^+ - (K-S_T)^+}{B-K}$. Whether S_T is bigger or smaller than B the result is always smaller or equal than 1.

Taking expectations and using the martingale property for the last term of the RHS, we obtain (4.2). We refer to [27] for the proof that there exists a martingale for which the bound is attained. □

Let us derive the optimal upper bound of a digital option.

Proposition 4.2. *Let $B > S_0$. The optimal upper bound consistent with market data of a digital option is given by:*

$$U_{dig} = \inf_{K<B} \frac{C(K)}{B - K} \tag{4.3}$$

The bound does not improve when the underlying is assumed to be continuous.

Proof. We adopt a similar reasoning as before to prove that (4.3) is the optimal bound. We bound the payoff from above, for every $K < B$:

$$\mathbb{1}_{\{H_B \leq T\}} \leq \frac{(S_T - K)^+}{B - K} + \frac{B - S_T}{B - K}\mathbb{1}_{\{H_B \leq T\}} \tag{4.4}$$

In the aim of proving the above inequality we distinguish once again the case where $H_B \leq T$ or not. If $H_B \geq T$ (i.e the barrier has been attained), the LHS of (4.4) is equal to 1 and the RHS is equal to 1 if $S_T \geq K$ and $\frac{B-S_T}{B-K}$ otherwise, either case the RHS is greater than or equal to 1. If the Barrier is not reached, the LHS is null and the RHS non-negative. Then, by taking expectation in (4.4) and using the martingale property for the last term in the RHS, we obtain for every $K < B$: $\mathbb{P}(H_B \leq T) \leq \frac{C(K)}{B-K}$. Let us point out that (4.4) can be interpreted with a super-replicating argument, The RHS refers to a strategy that consists of: a long position of $\frac{1}{B-K}$ Calls with strike K (and maturity T) and if the barrier is reached a short position of $\frac{1}{B-K}$ forward contracts (with strike B). Since the short position of the forward is costless, the cost of the hedging strategy is therefore the cost of $\frac{1}{B-K}$ Call options.

Finally by taking the infimum over all $K < B$ we obtain (4.3). To prove that it is actually the optimal upper bound, we refer to [27] for the existence of the martingale consistent with market data and for which the bound is attained.

□

4.3 Barrier options

In the previous section, we have seen how to derive optimal upper and lower bounds of digital options. Let us now outline similar results for other path-dependent derivatives commonly known as single barrier options, more specifically up-and-in and up-and-out Calls and Puts. Down-and-in and down-and-out barrier options can easily be deduced from "up" barrier options. We will see how to then derive optimal lower bounds using optimal upper bounds.

Just as before, our aim is to derive an astute super-replicating strategy to bound the payoff from above to then derive the upper price. Optimality is then shown by exhibiting a martingale in such a way that the upper bound is actually attained.

In this section, we do not assume that the underlying asset is continuous (allowing jumps). We will only provide a sketch of proof for the up-and-in Call, while other proofs are discussed in detail in [27] and [26].

4.3.1 Upper bounds of barrier Call options

The up-and-in Call with strike K and Maturity T has the same payoff of a Call if the underlying asset crosses the barrier B before T and has a null payoff otherwise. Formally, the payoff of an up-and-in Call is $(S_T - K)^+ \mathbb{1}_{\{H_B \leq T\}}$. Notice that if $K \geq B$, the payoff is the same as a simple Call option and, thus, we assume $B > K$.

Proposition 4.3. *Let us define* $a = \inf_{K<B} \frac{C(K)}{B-K}$ *(one can show that the infimum is attained). If* $a > K$*, the optimal upper bound price of an up-and-in Call is given by:*

$$\frac{B-K}{B-a} C(a) \tag{4.5}$$

and C(K) otherwise.

Proof. Let $s \in (K, B)$. We use the inequality:

$$(S_T - K)^+ \mathbb{1}_{\{H_B \leq T\}} \leq \frac{B-K}{B-s}(S_T - s)^+ + \frac{s-K}{B-s}(B - S_T)\mathbb{1}_{\{H_B \leq T\}} \tag{4.6}$$

Let us prove the above inequality. If $S_T \leq K$ or $H_B > T$, the LHS is zero and $(B - S_T)$ in the RHS is non-negative; therefore, the RHS is non-negative. If the LHS is non-negative (i.e $S_T - K > 0$ and $H_B \leq T$), then the RHS is equal to the LHS when $(S_T > s)$ and the RHS is strictly greater than the LHS when $K < S_T < s$.

Here again, (4.6) can have a super-replicating interpretation. It is the strategy that consists in buying $\frac{B-K}{B-s}$ Call options with strike s and, if the barrier is reached, shorting $\frac{s-K}{B-s}$ forward contracts with strike B.

Taking the expectation in (4.6) and using the martingale property for the last term (or saying that the short position on a forward contract is costless), we obtain that the price is bounded by

$\frac{B-K}{B-s}C(s)$ for every $s \in (K, B)$. The best bound is therefore obtained by minimizing the function $s \to \frac{B-K}{B-s}C(s)$ over all $s \in (K, B)$, which leads to the minimizer $s^* = min(a, K)$. The upper bound of the proposition 4.3 follows.

The optimality is then demonstrated by exhibiting a martingale for which the bound is attained. This is explained in detail in [27]. □

The payoff of an up-and-out Call with strike K and Maturity T is $(S_T - K)^+ \mathbb{1}_{\{H_B > T\}}$, it is the same as the one of a Call if the underlying does not reach the barrier B before T and zero otherwise. Again, if $K \geq B$ the option is worthless as the payoff is always equal to zero, we thus assume that $B > K$.

Proposition 4.4. *The optimal upper bound of an up-and-out Call is given by:*

$$C(K) - C(B) - (B - K)\mu([B, \infty)) = C(K) - C(B) + (B - K)C'(B)$$

This bound can be improved if we assume that the underlying asset process is continuous.

Proof. See [27, Proposition 3.2, page 296]. □

4.3.2 Lower bounds of Barrier Call options

Optimal lower bounds are obtained with previous results and using the parity relation:

$$(S_T - K)^+ \mathbb{1}_{\{H_B \leq T\}} = (S_T - K)^+ - (S_T - K)^+ \mathbb{1}_{\{H_B > T\}}$$

Proposition 4.5. *The lower optimal bound of an up-and-in Call is C(K) if $B \leq K$ and $C(B) - (B - K)C'(B)$ otherwise.*

The lower optimal bound of an up-and-out Call is equal to zero if $B \leq K$ or $a \leq K < B$ (where the notation of a is the same as before). If $B > a > K$ the lower bound is:

$$C(K) - \frac{B - K}{B - a}C(a)$$

4.3.3 Upper bounds for Barrier Puts

In this section we will state the optimal upper bounds of Barrier put options. The payoff of an up-and-in Put with strike K and maturity T is $(K - S_T)^+ \mathbb{1}_{\{H_B \leq T\}}$.

Proposition 4.6. *Let us define $\alpha = \sup_{K<B} \frac{C(B)-P(K)}{B-K}$ (one can show that this supremum is attained). The upper optimal bound of an up-and-in Put depends on whether $B > K$ or not. For $B > K$ the upper bound is P(K) if $\alpha > K$ and*

$$\frac{K - \alpha}{B - \alpha}C(B) + \frac{B - K}{B - \alpha}P(\alpha)$$

otherwise. For $K \geq B$, the optimal upper bound is:

$$C(K) + \frac{K-B}{B-a}C(a)$$

where a remains unchanged.

Proof. See [27, page 298] □

Notice that when the Barrier B is equal to the strike K, the price of the up-and-in Put is similar to a Call option with strike K. This can also be achieved with the following replicating strategy: long one call with strike K at initial time and if the underlying asset breaks the barrier B, short one forward contract (with strike K) on the underlying. If the barrier is reached before T, the payoff of the replicating portfolio is $(S_T - K)^+ + (K - S_T) = (K - S_T)^+$. If the barrier is not reached, the payoff remains null. The hedging strategy therefore offers exactly the same payoff as the up-and-in Put. Since the forward position is costless, the price of Barrier put is therefore the cost of the hedging strategy $C(K)$.

On the other hand, the payoff up-and-out Put is $(K - S_T)^+ \mathbb{1}_{\{H_B > T\}}$.

Proposition 4.7. *If $B > K$, the optimal upper bound of an up-and-out Put is P(K). Otherwise, it is $P(B) + (K-B)\mu((-\infty, B)) = P(B) + (K-B)(1 + C'(B))$.*

Proof. See [27, page 299] □

4.3.4 Lower bounds for Barrier Puts

Similarly, to derive optimal lower bounds for Barrier Puts, we use the following parity relation:

$$(K - S_T)^+ \mathbb{1}_{\{H_B \leq T\}} = (K - S_T)^+ - (K - S_T)^+ \mathbb{1}_{\{H_B > T\}}$$

Proposition 4.8. *The optimal lower bound of an up-and-in Put is 0 if $K < B$ and $P(K) - P(B) - (K-B)(1 + C'(B))$ otherwise.*

Concerning the optimal lower bound of an up-and-out Put. For $B > K$ the lower bound is 0 if $\alpha \geq K$ and

$$P(K) - \frac{K-\alpha}{B-\alpha}C(B) - \frac{B-K}{B-\alpha}P(\alpha)$$

otherwise. For $B \leq K$, it is:

$$K - S_0 - \frac{K-B}{B-a}C(a).$$

Proof. See [27, page 300] □

4.4 Numerical examples

4.4.1 Introduction

In this section, we will illustrate previous robust bound results with a few numerical examples. We assume that the initial spot price is equal to 1 and that all payoffs occur within 1 year: $S_0 = 1$ and T = 1.

We generate a volatility structure using the SVI model with parameters chosen randomly but in a way to reflect real market behaviour. Call prices are Black-Scholes one obtained with the latter volatility structure. These results are represented in Figure 18.

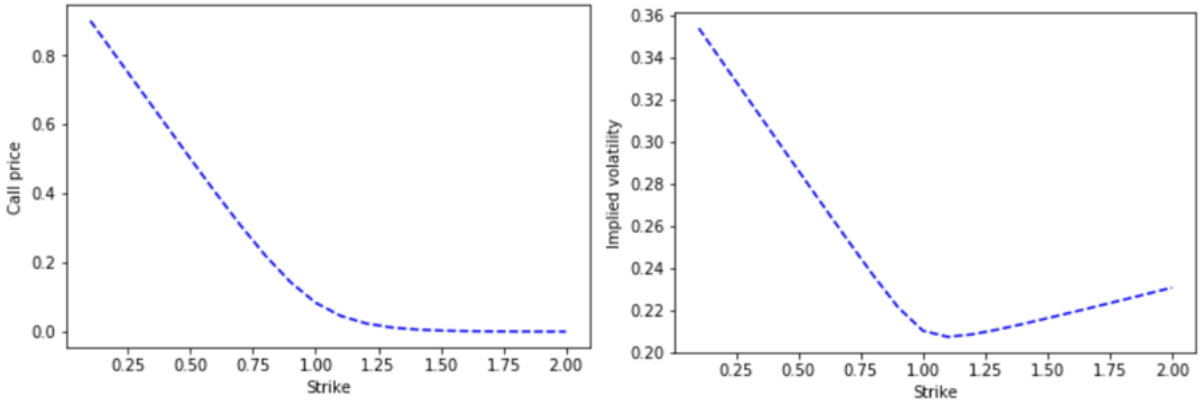

Figure 18: Simulated implied volatility structure and its according Black-Scholes prices

Put option prices can be obtained easily using the Put-Call parity.

Using the above Vanilla prices, the aim is to compute upper and lower bounds of Barrier options as seen in previous sections. Then, for comparison purposes, we will compute Barrier option prices with models that are consistent with market data and see whether or not the result indeed lies within the upper and lower bound. For the sake of this investigation, we will mainly use two models: Black-Scholes and square root CEV.

4.4.2 Black-Scholes framework

Let us first see whether the prices obtained with the Black-Scholes model are coherent with upper and lower optimal bounds. While recalling that the risk-free interest rate is zero, we assume that the underlying satisfies for each strike K:

$$\mathrm{d}S_t = \sigma(K) S_t \mathrm{d}t \tag{4.7}$$

where $\sigma(K)$ is the implied volatility for each Strike K as shown in Figure 18. By definition of the implied volatility, this model is consistent with available Vanilla prices. Under this framework,

we compute numerically the prices of Barrier options using a Monte-Carlo simulation with a finite-difference method to discretize the PDE (4.7). All the results are obtained with an average of M = 10000 paths and while allowing the underlying asset to take n=100 values between 0 and T.

Let us start with the up-and-in Call option. The knock-in barrier B is 1.04, we use the proposition 4.3 and 4.5 to compute upper and lower optimal bounds, $C'(B)$ is numerically approximated by $\frac{C(B+\epsilon)-C(B-\epsilon)}{2\epsilon}$ for ϵ is small enough (for instance $\epsilon = B/1000$), a and α are obtained using a simple minimization/maximization routine. Results are shown in Figure 19 for strikes ranging from 0.8 to 1.1.

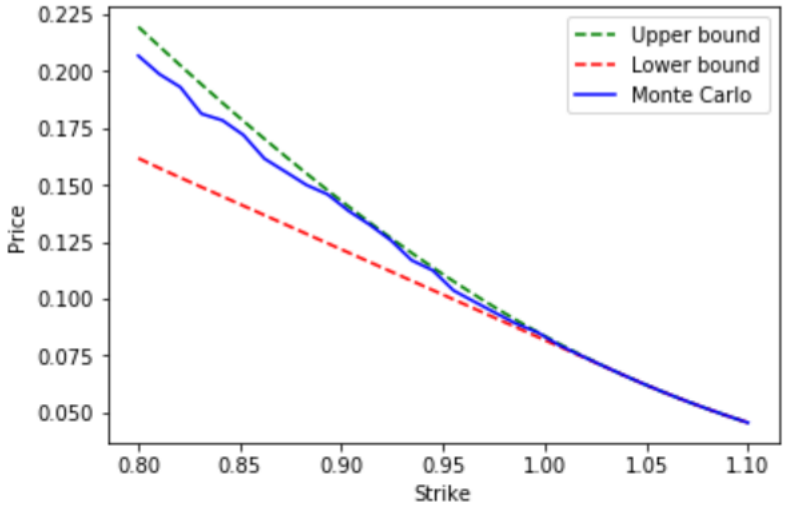

Figure 19: Optimal upper and lower bounds and Monte Carlo prices of up-and-in Call options. The knock-in barrier B = 1.04.

It should be noted that when the strike stands above the Barrier 1.04, the barrier feature is useless as the payoff is the same as a simple Call option. This is the reason why the upper, lower and Monte Carlo prices are all the same.

The results obtained for up-and-in put options are plotted in the Figure 20 for a fixed Barrier B = 1.04.

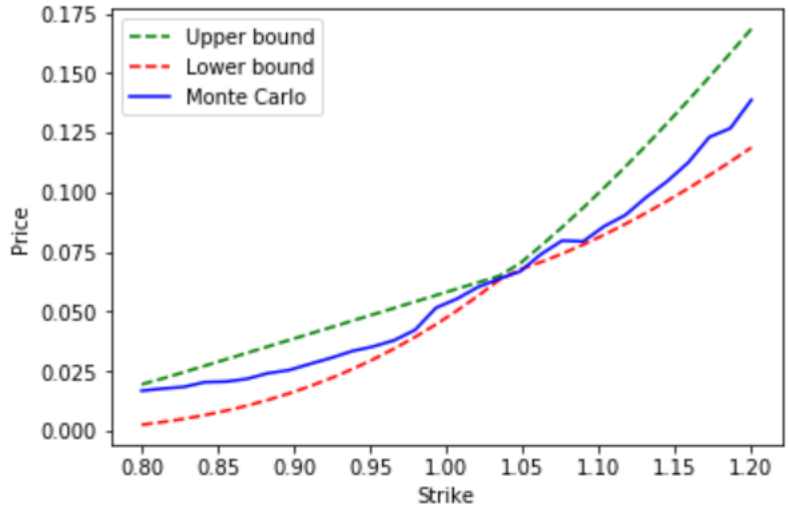

Figure 20: Optimal upper and lower bounds and Monte Carlo prices of up-and-in Put options. The knock-in barrier B = 1.04.

Let us highlight that near the barrier, the upper and lower band is the most narrowed and when the Barrier is equal to the Strike, the lower and upper bounds are simply equal to a Call option with the same Strike (see section 4.3.3).

For the up-and-out Call option, we assume that $B = 1.3 > K$ for every K, otherwise the option is worthless. The results obtained are summarized in following figure 21.

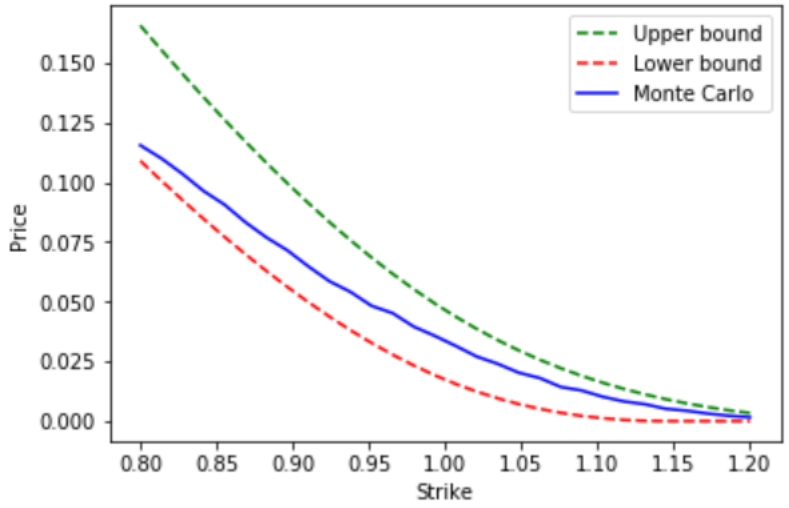

Figure 21: Optimal upper and lower bounds and Monte Carlo prices of up-and-out Call options. The knock-in barrier is B = 1.3 and is greater than all strikes

For the up-and-out Put option, we use a Barrier B equal to 1.05. The results are shown in figure 22.

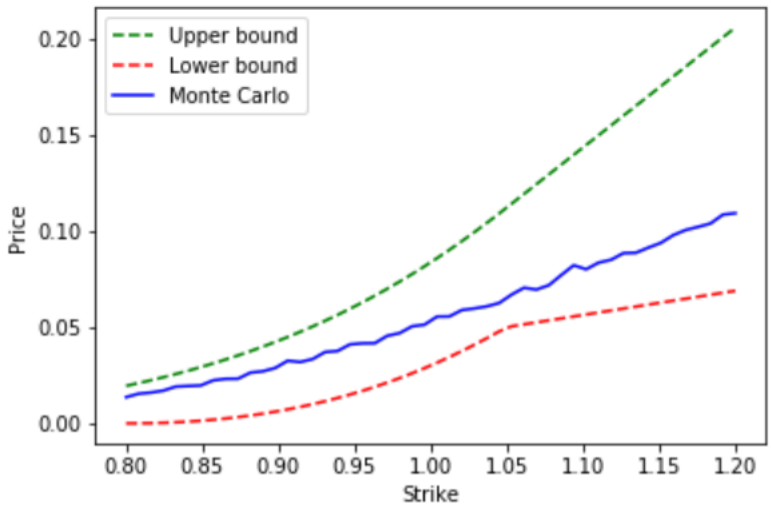

Figure 22: Optimal upper and lower bounds and Monte Carlo prices of up-and-out Put options. The knock-in barrier is B = 1.05

This the upper/lower bound is tighter for smaller strikes.

For all previous results, the Monte Carlo prices simulated numerically under the Black-Scholes framework lie within the upper and lower bounds. This result is in line with previous theoretical results since any model consistent with Vanilla market prices should satisfy this property. The next section will allow us to explore another model example.

But what happens if the model is not consistent with market data? For example, a naive approach in the Black-Scholes model is to use the same volatility σ for every strike. Generally, this volatility is taken to be the implied volatility calibrated with the at-the-money Call option. Let us however use the implied volatility of the Call with strike K=0.75 to have more striking results. Given the volatility skew before the ATM strike (see figure 18), we basically tend to over-price Calls with strike above 0.75 and under-price those with strike below 0.75. Therefore, this model is not consistent with market Data, which Figure 23 illustrates with the results obtained under this model for the case of up-and-in Call options with the same barrier as before (B = 1.04).

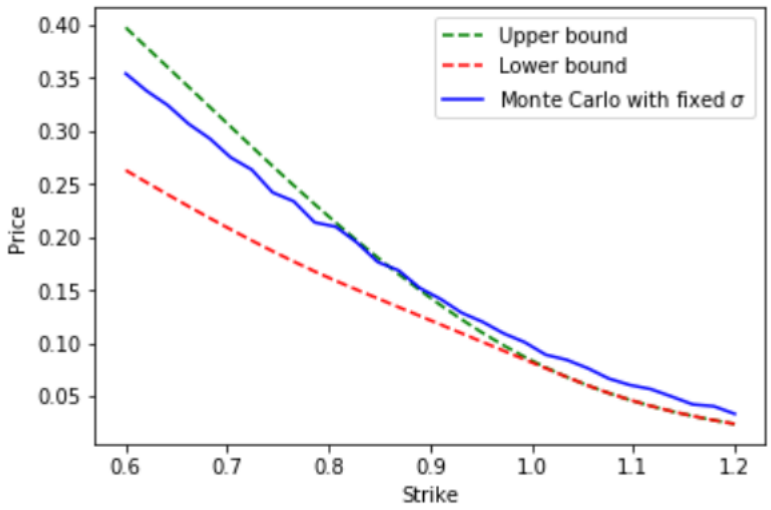

Figure 23: Optimal upper and lower bounds prices of up-and-in Call options. Monte Carlo prices are obtained with a fix σ corresponding to the implied volatility of the Call with strike K=0.75

This time, some Black-Scholes prices lie above the upper bound. This is why pricing naively under a Black-Scholes model with one single calibration leads to arbitrage opportunities.

4.4.3 Square root CEV framework

We will now study another model consistent with Vanilla prices and coherent with upper and lower optimal bounds. We consider the square root CEV model:

$$\mathrm{d}S_t = \sigma'(K)\sqrt{S_t}\mathrm{d}t, \tag{4.8}$$

where the CEV volatility $\sigma'(K)$ is calibrated for each strike in order for it to be consistent with available Call prices. The calibration is done through an optimization routine by minimizing the quantity $|C_{CEV}(K) - C_{Mkt}(K)|$ for each K, where C_{CEV} is the Call price with Strike K of the CEV model (obtained numerically with Monte Carlo simulations), and $C_{Mkt}(K)$ is the Call market price.

The simulation results obtained for up-and-out and up-and-in Call options respectively summarized in Figures 24 and 25. The simulated prices under the Square root model are in line with previous theoretical results since they lie within the optimal bound too.

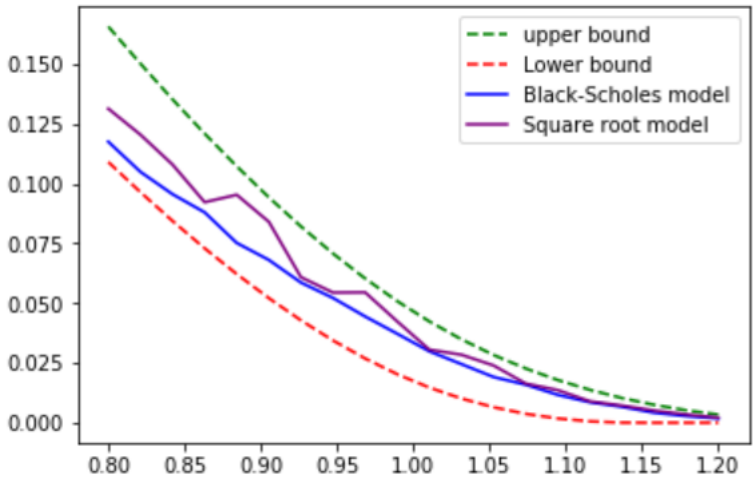

Figure 24: Monte Carlo simulation of Black-Scholes and Square root models for an up-and-out Call option. The knock-out barrier is B = 1.3

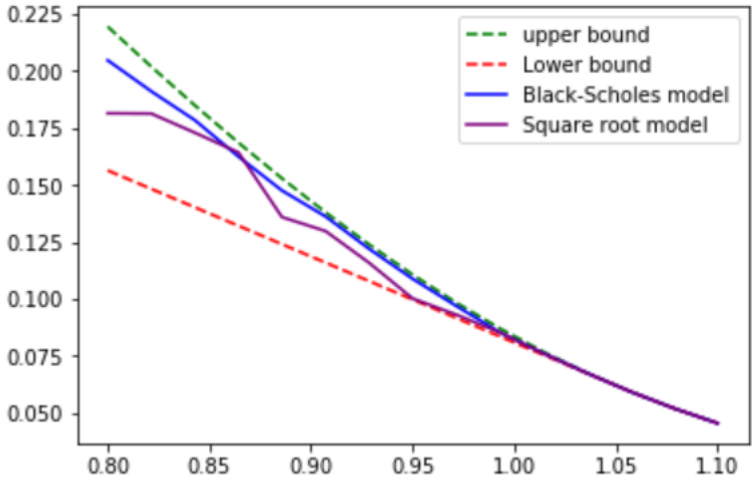

Figure 25: Monte Carlo simulation of Black-Scholes and Square root models for an up-and-in Call option. The knock-in barrier is B = 1.04.

4.5 Conclusion

In this chapter, we outlined robust methods to price Digital and Barrier path-dependent options. Using astutely upper and lower bound for the payoff, we then saw how the knowledge of Vanilla prices allows us to produce optimal bounds. Finally, we verified these bounds numerically using two models that are consistent with market data.

Conclusion

In this thesis, we explored a few methods of robust pricing. In an environment where regulators are very demanding regarding model risk, these methods seem to provide alternative ways to reduce and manage the risk effectively.

We firstly saw how uncertain volatility models offer a way around autoregressive or stochastic models for the volatility process. Then, we outlined optimal transport problems and how they can be applied to robust pricing. Finally, we studied robust methods for specifically Barrier and Digital path-dependent options.

All these methods are exogenous and use market Vanilla prices to provide robust and optimal upper/lower bounds. However, the less model assumptions, the wider the upper/lower bounds spread. Robustness can therefore produce large bounds that are without any practical use. For instance in the second chapter, we saw that the λ-UVM, which calibrates the parameters σ_{min} and σ_{max} and assumes that the discounted stock process has no jumps and is a martingale with respect to the Brownian Motion filtration, gives narrower upper/lower bounds compared to MOT (which is based on fewer assumptions). It is therefore important to compromise between robustness and model assumptions in order to produce optimal bounds that decrease model risk and are still used in practice.

Numerical methods covered in this paper are mainly based on a discrete-time framework. Continuous-time versions would be an interesting topic to explore as they lead to even tighter and robust bounds.

References

[1] D. Baker. *Martingales with specified marginals*. Pierre et Marie Curie university PhD thesis, 2012.

[2] M. Beiglböck, M. Nutz and N. Touzi. *Complete Duality for Martingale Optimal Transport on the Line*. Academic Press, 2016.

[3] P. Henry-Labordère. *Model-free Hedging: A Martingale Optimal Transport Viewpoint*. Book, 2017.

[4] M. Avellaneda, A. Levy and A. Parás. *Pricing and Hedging Derviative Securities in Markets With Uncertain Volatilities*. Academic Press, 1995

[5] M. Avellaneda and A. Parás. *Managing the volatility risk of portfolio of derivative securities: the Lagrangian uncertain volatility model*, 1996

[6] T. J. Lyons *Uncertain volatility and the risk-free synthesis of derivatives*. Academic Press, 2006.

[7] N. El Karoui and M. Quenez *Dynamic Programming and Pricing of Contingent Claims in an Incomplete Market*. Journal of Control and Optimization, 1995.

[8] P. Hagan, D. Kumar, A. Lesniewski and D. Woodward *Managing Smile Risk*. Wilmott magazine, page 85, 2002.

[9] A. Parás *Non-Linear partial differential equations in finance: a study of volatility risk and transaction costs*. Ph.D thesis at New York university, 1995

[10] G. Carlier *On a class of multidimensional optimal transport problems*. Journal of Convex Analysis, 2003.

[11] B.Acciaio, M.Beiglböck, F.Penkner and W.Schachermayer *Model free version of the fundamental theorem of asset pricing and the super replication theorem.* Academic Press, 2013

[12] L. Denis and C. Martini *A Theoretical framework for the pricing of contingent claims in the presence of model uncertainty*. Annals of Applied probability, 2006.

[13] Y. Dolinsky and H.M. Soner *Robust hedging and martingale optimal transport in continuous time*. Academic Press, 2014.

[14] G. Monge *Mémoire sur la théorie des déblais et des remblais*. Imprimerie Royale, 1781.

[15] L. V. Kantorovich *On the Translocation of Masses*. Proceedings of the USSR Academy of Sciences, 1942.

[16] M. Beiglböck, P. Henry-Labordère and F. Penkner *Model-independent bounds for option prices: a mass transport approach.* Academic press, 2011.

[17] N.Touzi *Optimal transportation under controlled stochastic dynamics and bounds on derivatives.* Journée d'inauguration, 2012.

[18] D. Hobson *The Skorokhod Embedding Problem and Model-Independent Bounds for Option Prices*, 2010

[19] A. Fahim and Y.J. Huang *Model-independent superhedging under portfolio constraints.* Academic Press, 2016.

[20] C. Villani: *Topics in optimal transport.* Book, 2003.

[21] V. Strassen *The existence of probability measures with given marginals.* Page 423-439, 1965.

[22] D.T. Breeden and R.H. Litzenberger *Prices of state-contingent claims implicit in options prices.* Press J. Business, 1978.

[23] P. Henry-Labordère and N. Touzi *An explicit martingale version of Brenier's theorem*, 2016.

[24] G.Guo and J. Oblój *Computational methods for martingale optimal transport problems.* Academic Press, 2017.

[25] D. Gilat and L.E. Dubins *On the distribution of maxima of martingales.* 1978.

[26] D. Hobson *The Minimum Maximum of a Continuous Martingale with given initial and terminal laws.* Journal article, 2002.

[27] H. Brown, D. Hobson and L.C.G. Rogers *Robust hedging of barrier options*, 2001.

[28] J. Gatheral and J. Antoine *Arbitrage-free SVI volatility surface*, 2016.

[29] D. Breeden and R. Litzenberger *Prices of State Contingent Claims implicit in Option Prices.* The journal of Business, 1978.

[30] P. Carr and R. Lee *Robust replication of volatility derivatives.* Academic Press, 2009.

[31] P. Henry-Labordère, J. Obłój, P. Spoida and N. Touzi *The maximum maximum of a martingale with given marginals.* Academic Press, 2016.